OPEN ACCESS

Original research

A novel peptide protects against diet-induced obesity by suppressing appetite and modulating the gut microbiota

Zhanzhan Li,[1,2] Bing Zhang,[1,2] Ning Wang,[1,2] Zhenqiang Zuo,[1] Hong Wei,[3] Fangqing Zhao [1,2,4,5]

ABSTRACT

Objective The obesity epidemic and its metabolic complications continue to be a major global public health threat with limited effective treatments, especially drugs that can be taken orally. Peptides are a promising class of molecules that have gained increased interest for their applications in medicine and biotechnology. In this study, we focused on looking for peptides that can be administrated orally to treat obesity and exploring its mechanisms.

Design Here, a 9-amino-acid peptide named D3 was designed and administered orally to germ-free (GF) mice and wild-type (WT) mice, rats and macaques. The effects of D3 on body weight and other basal metabolic parameters were evaluated. The effects of D3 on gut microbiota were evaluated using 16S rRNA amplicon sequencing. To identify and confirm the mechanisms of D3, transcriptome analysis of ileum and molecular approaches on three animal models were performed.

Results A significant body weight reduction was observed both in WT (12%) and GF (9%) mice treated with D3. D3 ameliorated leptin resistance and upregulated the expression of uroguanylin (UGN), which suppresses appetite via the UGN-GUCY2C endocrine axis. Similar effects were also found in diet-induced obese rat and macaque models. Furthermore, the abundance of intestinal *Akkermansia muciniphila* increased about 100 times through the IFNγ-Irgm1 axis after D3 treatment, which may further inhibit fat absorption by downregulating Cd36.

Conclusion Our results indicated that D3 is a novel drug candidate for counteracting diet-induced obesity as a non-toxic and bioactive peptide. Targeting the UGN-GUCY2C endocrine axis may represent a therapeutic strategy for the treatment of obesity.

WHAT IS ALREADY KNOWN ON THIS TOPIC

⇒ Uroguanylin (UGN) is an anorexic hormone that can target the GUCY2C receptor of the hypothalamus and activate anorexigenic pathways.

⇒ Regulation of the gut microbiota can improve host metabolism and reduce obesity.

⇒ Polypeptides such as glucagon-like peptide-1 (GLP-1) analogue used to prevent obesity represents a new direction for drug design, but with poor adherence of patients to injectable therapies.

WHAT THIS STUDY ADDS

⇒ Oral administration of D3, a 9-amino-acid peptide but not a GLP-1 analogue, can counteract diet-induced obesity in mice, rat and rhesus macaca.

⇒ D3 can effectively inhibit appetite through the UGN-GUCY2C endocrine axis.

⇒ D3 restores the gut microbiota disorder caused by obesity and specifically increases the abundance of *Akkermansia muciniphila* in the gut via the IFNγ-Irgm1 axis.

HOW THIS STUDY MIGHT AFFECT RESEARCH, PRACTICE OR POLICY

⇒ D3 is a promising candidate of weight reducing drug that can be taken orally to manage excess weight and obesity.

⇒ The UGN-GUCY2G axis represents a potential therapeutic target for the development of anti-obesity drugs.

INTRODUCTION

According to the WHO, 650 million adults had obesity in 2016, and 39 million children under the age of 5 were overweight or obese in 2020.[1] Obesity is becoming a worldwide epidemic and poses major therapeutic challenges due to its associated high risk for developing non-communicable diseases, including type 2 diabetes, cardiovascular disease, stroke, cancer and depression.[2] Obesity is also linked with decreased life expectancy and increased morbidity and mortality and economic burden on healthcare systems.[3] Various strategies have been developed to combat obesity and overweight conditions, especially through reducing energy intake or enhancing metabolic expenditure rate. However, recent studies found that excessive dietary interventions may lead to physical and mental health disorders,[4] which further increase the demand for effective, safe and acceptable therapeutic options.

Extensive studies have shown that obese humans and mice display an altered gut microbiota with reduced diversity and increased capacity to absorb energy.[5] The intestinal microbiota is essential in regulating host energy homeostasis, fat accumulation and mucosal barrier integrity.[6] Disordered microbiota are closely associated with metabolic

► Additional supplemental material is published online only. To view, please visit the journal online (http://dx.doi.org/10.1136/gutjnl-2022-328035).

[1]Beijing Institutes of Life Science, Chinese Academy of Sciences, Beijing, China
[2]University of Chinese Academy of Sciences, Beijing, China
[3]Laboratory Animal Department, College of Basic Medicine Army Medical University, Chongqing, China
[4]Center for Excellence in Animal Evolution and Genetics, Chinese Academy of Sciences, Kunming, China
[5]Key Laboratory of Systems Biology, Hangzhou Institute for Advanced Study, University of Chinese Academy of Sciences, Hangzhou, China

Correspondence to
Professor Fangqing Zhao, Beijing Institutes of Life Science, Chinese Academy of Sciences, Beijing 100045, China; zhfq@biols.ac.cn
Professor Hong Wei; weihong63528@163.com

ZL and BZ are joint first authors.

Received 10 June 2022
Accepted 28 June 2022
Published Online First 8 July 2022

Linked

► http://dx.doi.org/10.1136/gutjnl-2022-328158

Check for updates

To cite: Li Z, Zhang B, Wang N, *et al*. *Gut* 2023;**72**:686–698.

disorders such as obesity, insulin resistance and glucose intolerance.[7] Intervention strategies that modulate the gut microbiota have been proposed to prevent and treat obesity. For example, tempol can decrease the weight gain of mice by preferentially reducing the genus *Lactobacillus*.[8] Cranberry extract[9] and metformin[10] can protect mice from diet-induced obesity by increasing *Akkermansia muciniphila* in the gut microbiota. Several recent studies have shown that daily administration of *A. muciniphila* can counteract the development of high-fat-diet (HFD)-induced obesity.[11] Additionally, oral gavage with either *Bacteroides thetaiotaomicron*[12] or *Lactobacillus rhamnosus GG*[13] can also alleviate diet-induced body weight gain and adiposity in mice.

Consisting of 20 natural amino acids and a multitude of non-natural amino acids, peptides have attractive pharmacological profiles, excellent safety and tolerability, which represent an excellent starting point for the design of novel therapeutics.[14] Currently, a number of peptides have been developed to prevent obesity, such as glucagon-like peptide-1 (GLP-1),[15] atrial natriuretic peptide and brain natriuretic peptide.[16] Many of these peptides, however, are usually longer than 20 amino acids and are therefore less likely to escape degradation by proteases in the gastrointestinal tract. On the other hand, recent studies on apelin[17] and semaglutide[18] indicate that oral drugs represent the trend in weight-loss drug development for the preference of general patients for oral medicines compared with injectable therapies. In addition, small molecules may have some intrinsic disadvantages, including the accumulation of peptides in organs and potential toxic metabolic products causing side effects.[19] Most of the peptides are membrane impermeable, which makes the therapeutic application of them restricted to extracellular and transmembrane targets, and the inability to permeate the intestinal mucosa necessitates parenteral administration via subcutaneous or intravenous injection, with the corresponding detriment to patient convenience and compliance. Based on the principle of biocompatibility, improving the hydrophobicity of peptides can improve their ability to interact with cell surface receptors and even promote their penetration of the membrane and binding to internal targets.[20] Further studies are still needed to find or modify more endogenous peptides that are much smaller and lack cumulative toxicity for the treatment of obesity.

In this study, we designed and optimised a 9-amino-acid peptide with high hydrophobicity from human α-defensin 5 (HD-5), which was found to reverse dyslipidaemia and improve glucoregulatory capacity in diet-induced obese (DIO) mice through feeding directly mixed with feed.[21] By using both pharmacological and genetic approaches, we identified and confirmed the role and mechanism of the modified peptide (D3) in inhibiting obesity development. Metabolic analysis revealed that D3 can ameliorate insulin and leptin resistance. By performing 16S rRNA amplicon sequencing and faecal microbial administration experiments, we observed increased abundance of gut commensal *A. muciniphila* and a causal relationship between it and the reduced anabolism of adipose tissue. Our study reports a new and promising candidate drug with high safety that can be taken orally for the prevention and treatment of obesity.

RESULTS

Oral administration of D3 counteracts obesity

Increasing electric charge and hydrophobicity can improve the membrane permeability of peptides. Therefore, to enhance hydrophobicity, four peptides named D1–4 were modified from one of the fragments of HD5 degraded by proteases in human duodenal fluid, HD5(1–9), the first nine amino acids at the N-terminus of defensin HD5.[22] All these peptides have a positive charge, among which D3 shows the strongest potential to penetrate cell membranes (online supplemental table 1 and figure 1A). We then evaluated the cytotoxicity of D1–4 in mammalian cells. D1–3 showed a slight inhibition of cell activity (2.71%–5.42%) at a very high concentration (2^9 μM), indicating their low cytotoxicity (online supplemental figure 1a). Additionally, D1–4 was assayed for potential toxic effects on mouse red blood cells in vitro. As shown in online supplemental figure 1b, the haemolytic rate of D1–4 at 2^8 μM was 1.06%–3.61%, respectively, indicating their low haemolytic effect. Therefore, the safe concentration range of these small peptides was set to 0–2^7 μM.

We next compared the effects of daily administration of D1–4 on HFD-fed mice. Strikingly, HFD-fed mice orally administered D3 rather than other peptides caused a 12.06%±2.35% decrease in body weight gain compared with the HFD-fed control mice over 8 weeks of HFD exposure (figure 1B–D). Recent findings indicate that obesity and its accompanying metabolic state are increasingly implicated in the composition of the gut microbiota.[1] To examine whether the gut microbiota may contribute to this effect, the same experiment was repeated in gnotobiotic (antibiotic cocktail, ABX) and germ-free (GF) mice. Similarly, 9.65%±4.26% and 9.14%±2.93% weight loss was observed in ABX (online supplemental figure 1C) and GF mice (figure 1D), respectively, suggesting that the reduction in adiposity by D3 oral gavage may be partially independent of the gut microbiome.

When challenged with additional insulin and glucose, D3-treated mice showed similar kinetics for glucose clearance as mice in the NC group, indicating that D3 could reduce the insulin resistance caused by obesity (figure 1E,F). Significant decreases in the tissue weight of inguinal, epididymal and perirenal fat were detected after D3 treatment ($p<0.05$, Wilcoxon test), which may be attributed to the reduced volume of fat cells (figure 1H). Additionally, D3 treatment also protected the liver from steatosis (figure 1H).

Based on these findings, we further examined the impact of 4 weeks of oral administration of D3 in a new cohort of DIO mice ($n=5$) after 10 weeks of HFD feeding. A significant reduction in body weight was observed in DIO mice ($p<0.01$, Wilcoxon test) (figure 1I), whereas the trend tended to be modest in the lean mice ($n=5$) fed a chow diet for 10 weeks in parallel ($p<0.05$, Wilcoxon t-test) (figure 1J). Notably, similar effects were observed after exchanging their diets at the 14th week (figure 1I,J). Taken together, these findings indicated that D3 treatment can prevent the onset and worsening of DIO, particularly on a HFD (online supplemental figure 1e).

D3 maintains energy homeostasis by inhibiting appetite

Considering that obesity occurs when energy intake exceeds energy expenditure, we therefore evaluated whether oral administration of D3 could affect food intake and/or energy metabolism. Notably, both in the specific pathogen-free (SPF) mice and the GF mice, D3 treatment significantly reduced food intake over time, with a significant reduction in 24-hour food intake compared with vehicle-treated animals ($p<0.05$, Wilcoxon test) (online supplemental figure 1d and figure 2A,B). In addition, indirect calorimetry analysis was performed to address whether changes in energy expenditure contributed to the observed D3-mediated weight loss. As shown in figure 2C, there was almost no difference in energy expenditure between the two groups ($p>0.05$, Wilcoxon test), indicating that D3 treatment

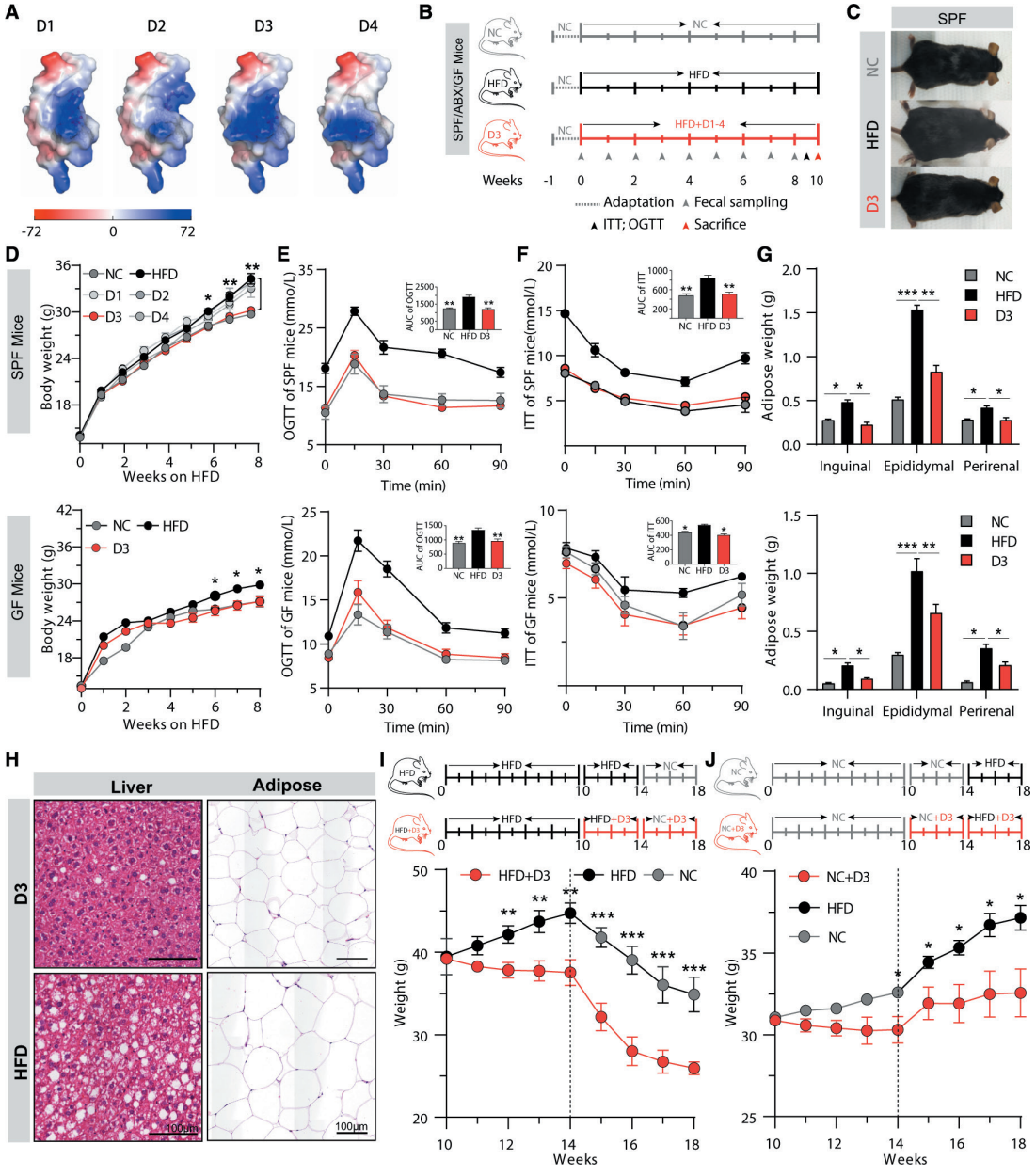

Figure 1 Oral administration of D3 counteracts obesity. (A) Design of HD5(1–9)-derived peptides D1–4 and their amphipathic surface. Blue, red and white represent positive, negative and neutral charges, respectively. Molecular models were generated with PyMOL 3.0. (B) Experimental outline. (C–H) Mice were divided into three groups (normal chow (NC), high-fat-diet (HFD) and D3) and fed a standard normal chow diet or 60% fat diet for 10 weeks; the D3 group was gavaged orally with D3, while saline was used as a parallel control (HFD). (C) Representative pictures of specific pathogen-free (SPF) mice at the eighth week. Mice in the D3 group exhibited reduced weight and better grooming. (D–F) SPF is shown on top and germ-free (GF) is shown on bottom. (D) Grams of weight gain measured over time, starting at 4 weeks of age; SPF mice (n=10–12 per group); GF mice (n=6–8 per group). Representative of three independent experiments. (E, F) insulin tolerance test (ITT) (E) and oral glucose tolerance test (OGTT) (F) of SPF mice and GF mice. (G) Total weight of white fat content in tissues from different organs. Representative of three independent experiments. (H) H&E staining of liver and epididymal fat from mice in the HFD or D3 group, taken at ×20 magnification. Scale bars: 100 μm. n=10 for each group. (I, J) Experimental outline (above); grams of weight gain measured over time, starting at 4 weeks of age, and the feed was changed at the 14th week. For D–G, I, and J, p values were determined by a two-tailed Wilcoxon test, and data are presented as the means±SEM; *p<0.05; **p<0.01; ***p<0.001.

may affect energy intake rather than energy expenditure. Pair-feeding was performed to explore the effects of lower food overload. As a result, mice orally administered D3 caused a 10.04%±2.19% (p<0.01, Wilcoxon test) decrease in body weight gain compared with the HFD control mice over 8 weeks of HFD exposure (figure 2D). Additionally, mice in the pair-fed group caused a 6.02%±2.03% decrease in body weight gain. These results suggest that the physiological effects of D3 are largely based on the inhibitory on appetite in mice.

To further explore the mechanism of D3, FITC-labelled D3 (FITC-D3) was used to visualise its systemic distribution in mice. Three hours after oral administration of FITC-D3 or FITC, intense fluorescence was visible in the intestinal tract of FITC-D3-treated mice, especially in the distal small intestine, but not

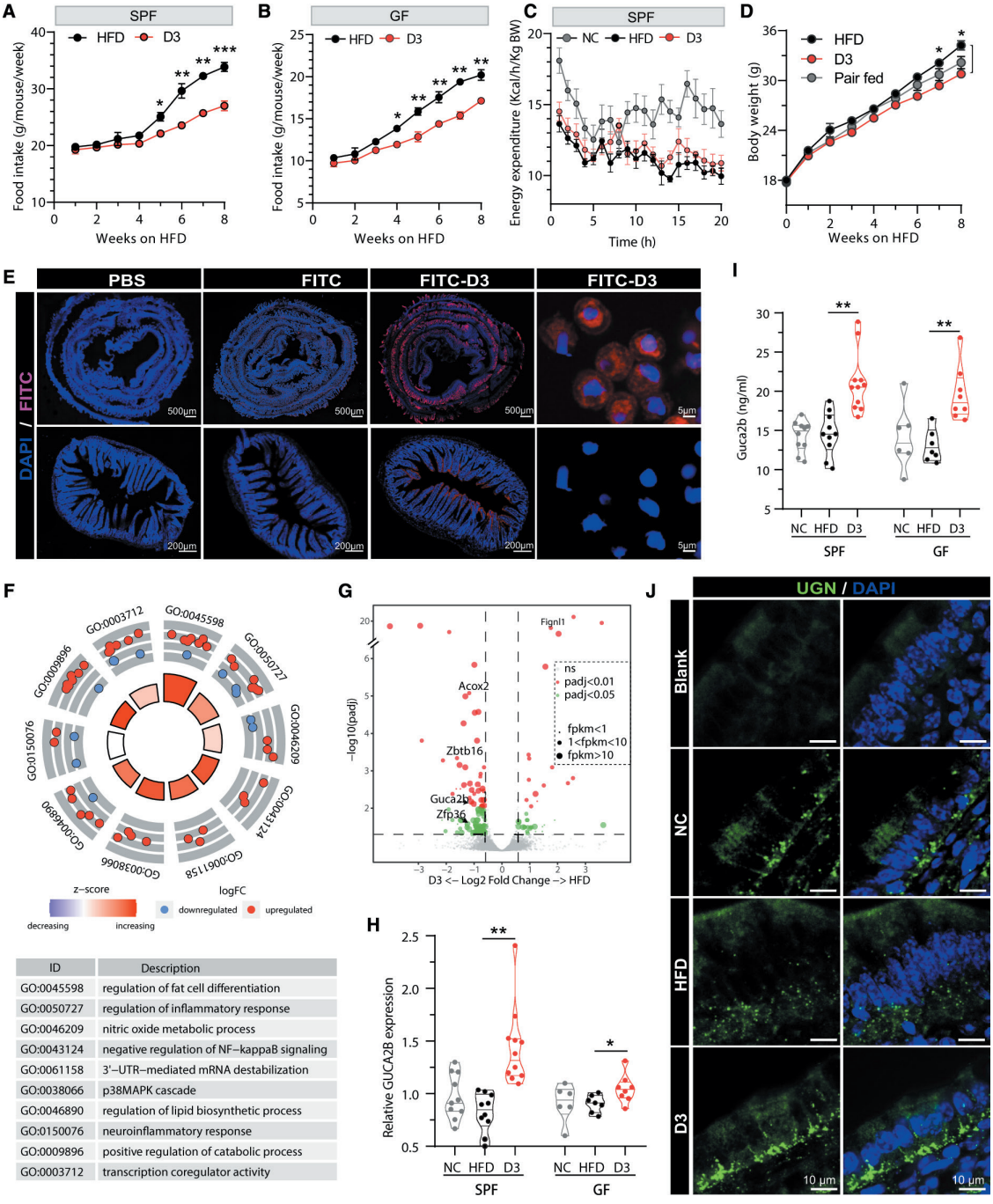

ID	Description
GO:0045598	regulation of fat cell differentiation
GO:0050727	regulation of inflammatory response
GO:0046209	nitric oxide metabolic process
GO:0043124	negative regulation of NF–kappaB signaling
GO:0061158	3'–UTR–mediated mRNA destabilization
GO:0038066	p38MAPK cascade
GO:0046890	regulation of lipid biosynthetic process
GO:0150076	neuroinflammatory response
GO:0009896	positive regulation of catabolic process
GO:0003712	transcription coregulator activity

Figure 2 D3 treatment decreases food intake by upregulating uroguanylin (UGN) expression in the ileum. (A, B) Food intake was measured once a week. (C) Effect of D3 treatment on acute food intake, which was measured every other day for 1 week. For A and B, (A) (specific pathogen-free (SPF) mice, n=10–12), (B) (germ-free (GF) mice, n=6–8). (C) Energy expenditure of SPF mice measured for 20 hours (n=6 mice/group). (D) Grams of weight gain measured over time in mice of pair-feeding, starting at 4 weeks of age (n=6 mice per group). (E) Localisation of FITC-labelled D3 visualised by confocal microscopy. The cell nucleus was stained with DAPI (blue). Swiss rolls (above, scale bars: 500 μm) and intestinal cross sections (below, scale bars: 200 μm) of SPF mice were obtained after 3 hours of oral administration. The last column shows the localisation of FITC-D3 after 1 hour of coincubation with HCT cells. The magenta colour presented by FITC is a pseudocolour that was replaced later to distinguish it from the immunofluorescence staining of UGN. Images are representative of three independent experiments with similar results. (F) RNA sequencing and KEGG pathways of genes in the ileum. (G) Volcano plot showing relative gene expression in the D3-treated group versus the HFD control group. All genes were plotted, and each circle represents one gene. The diameter of the circle represents the value of FPKM, p<0.05 (green) and p<0.01 (red). The X-axis shows the log2-fold change, and the Y-axis shows the –log10 of the p values. (H) Relative Guca2b mRNA levels in the ileum of mice gavaged with D3 or phosphate buffered saline (PBS). (I) The concentration of UGN (Guca2b protein) (ng/mL) in the serum of mice was determined by ELISA. (J) Double immunofluorescence in ileal sections for UGN (green dots located at the base of intestinal epithelial cells) and nuclei (blue). The diffuse green thin layer refers to background noise. Scale bars: 10 μm. For A, B, H and I, p values were determined by a two-tailed Wilcoxon test, and data are presented as the means±SEM; *p<0.05; **p<0.01; ***p<0.001.

in the mice of the FITC group (figure 2E). No distribution of FITC-D3 was observed in other organs (heart, spleen, lungs and kidneys), except slightly in the liver (figure 2E and online supplemental figure 2a). After 24 hours of FITC-D3 treatment, no fluorescence was observed in any of the above organs, including the intestines. These findings suggest that the major target of D3 is the distal small intestine, and its half-life is short.

Rich in arginine and lysine residues, some small peptides have remarkable cellular uptake ability to bind intracellular targets or to deliver electrostatically bioactive agents into cells.[23] To determine whether D3 can penetrate the cell membrane, HCT cells were coincubated with 10 μM FITC-D3/FITC for 2 hours. Confocal microscopy showed that FITC-D3 was homogeneously distributed in the cytosol of HCT cells and displayed a significantly higher fluorescence intensity than FITC (figure 2E and online supplemental figure 2b), implying enhanced cell uptake after conjugation with D3. The high efficiency of D3 in penetrating the membrane supports its potential to function as an intracellular regulator.

Subsequently, we investigated whether D3 could regulate the expression of genes in the distal small intestine of mice by using transcriptome analysis. Gene set enrichment analysis indicated that several KEGG pathways involved in metabolic and inflammatory responses, including the regulation of fat cell differentiation, positive regulation of catabolic process and negative regulation of I-kappaB kinase/NF-kappaB signalling, were the most significantly enriched pathways within D3-treated mice compared with HFD controls (figure 2F). Moreover, differential expression analysis identified 121 upregulated genes in the ileum of D3 mice ($p<0.05$, Wald test). Several genes involved in the regulation of lipolysis, including Zbtb16[24] and Acyl-CoA Oxidase 2 (Acox2),[25] and the inflammatory inhibition-related gene Zfp36[26] were validated by real-time quantitative PCR, particularly the Guca2b gene (adjusted $p<0.01$) (online supplemental figure 3b-d and figure 2G). Similar results were also found in adipose tissue: D3 treatment increased the mRNA expression of markers of adipocyte differentiation (eg, CCAAT/enhancer-binding protein-α, encoded by Cebpa) and lipid oxidation (eg, Acox2) and downregulated lipogenesis markers (eg, fatty acid synthase, encoded by Fasn) (online supplemental figure 3b). Previous studies revealed that Guca2b can act as a regulator of body weight homeostasis by modulating food intake through the UGN-GUCY2C endocrine axis.[27] We further verified the changes in UGN levels in serum by ELISA. Notably, D3 treatment significantly upregulated the expression of UGN in both SPF mice and GF mice ($p<0.01$, Wilcoxon test), as assessed by immunofluorescence (figure 2H–J and online supplemental figure 3e).

Intact leptin signalling contributes to the anti-obesity effect of D3

We sought to identify whether D3 treatment could protect against obesity in genetically obese (ob/ob) mice. As shown in figure 3A, no significant difference was observed in the body weight gain of the ob/ob mice between the D3 group and the HFD group after 6 weeks of oral administration. To validate that the anti-obesity effect of D3 was leptin associated, we next retrospectively examined the changes in leptin expression in SPF mice treated in previous experiments. Indeed, consistent with previous reports,[28] feeding an HFD significantly upregulated the expression of leptin in both SPF and GF mice, which could be restored by oral administration of D3 ($p<0.05$, Wilcoxon test) (figure 3B). To further demonstrate that D3 can ameliorate the leptin resistance, we first investigated the response of body weight to leptin administration by using an acute method, in which WT mice were treated with leptin intraperitoneally for 3 days, and then their body weight change was determined. As shown in figure 3C,A, marked body weight reduction was observed in the mice that received D3 after exogenous leptin treatment ($p<0.05$, Wilcoxon test) but not in the mice of the HFD group. Second, we detected the leptin-stimulated cytokines, including signal transducer and activator of transcription 3 (STAT3) and phosphatidylinositol 3-kinase (PI3K) pathways.[29] We found that within the negative regulators of leptin signalling, there was no significant difference in the mRNA expression level of PTB1B (online supplemental figure 4b) between the HFD and D3 groups, but SOCS-3 was significantly downregulated in D3-treated mice. The overexpression of SOCS-3 was found to inhibit leptin-induced pSTAT3 in vivo and consequently caused leptin resistance.[30] In contrast, the expression level of PI3K, whose level is positively correlated with the total expression level and can reflect the leptin sensitivity,[31] was significantly upregulated, which may represent an enhanced response to leptin (online supplemental figure 4b). Taken together, these results suggest that D3 treatment can restore leptin-induced signalling pathways in DIO mice and the leptin sensitivity.

We observed that leptin treatment caused a marked tendency towards a reduction in body weight in ob/ob mice, and leptin+D3 induced a more significant reduction than D3 alone (figure 3D), implying that supplementation with exogenous leptin can restore the function of D3 in ob/ob mice. Then, we quantified and compared the expression level of Guca2b in the ileum of ob/ob mice with that of WT mice. A 2.22-fold increase in the expression of Guca2b was observed after D3 treatment in ob/ob mice (OB-D3) compared with untreated ob/ob mice (OB-NC), whereas the WT mice of the SPF-D3 group achieved a 3.67-fold increase (figure 3E). Furthermore, ob/ob mice treated with leptin alone (OB-Lep) showed a 2.12-fold increase, which was lower than those treated with leptin+D3 (OB-Lep+D3, 3.46-fold increase) (figure 3E), indicating the synergistic effect of leptin and D3 on regulating the expression of UGN. The expression of UGN in the ileum of ob/ob mice treated with D3, leptin and D3+leptin was further visualised and verified by immunofluorescence (figure 3F). Taken together, these findings indicate that leptin may play a significant role in mediating the anorexigenic and anti-obesity effects of D3.

Some neurons in the hypothalamus associated with appetite are activated on fasting, which is accompanied by dramatic induction of c-Fos expression in these neurons.[32] To observe the effect of D3 treatment on the appetite of mice, 8-week-old SPF mice were gavaged with D3 or vehicle (saline) at 10:00 a.m. Transcardial and c-Fos staining were subsequently performed every 1 hour for 3 hours. The expression of c-Fos increased significantly at 1 hour after D3 administration, and then gradually returned to the normal level (online supplemental figure 4c), which was confirmed by subsequent immunofluorescence staining (figure 3H,J). We further measured the expression of AgRP and POMC during this process to identify the population of hypothalamic neurons implicated in the observed effects. The expression of POMC was significantly improved at 2 and 3 hours after D3 administration ($p<0.05$, Wilcoxon test), but with no significant changes in AgRP ($p>0.05$, Wilcoxon test) (figure 3G,K). Moreover, the colocalisation of c-Fos and POMC expressing neurons was observed in arcuate nucleus (figure 3H,I). These results suggest that D3 administration may indirectly affect POMC neurons in arcuate nucleus, which

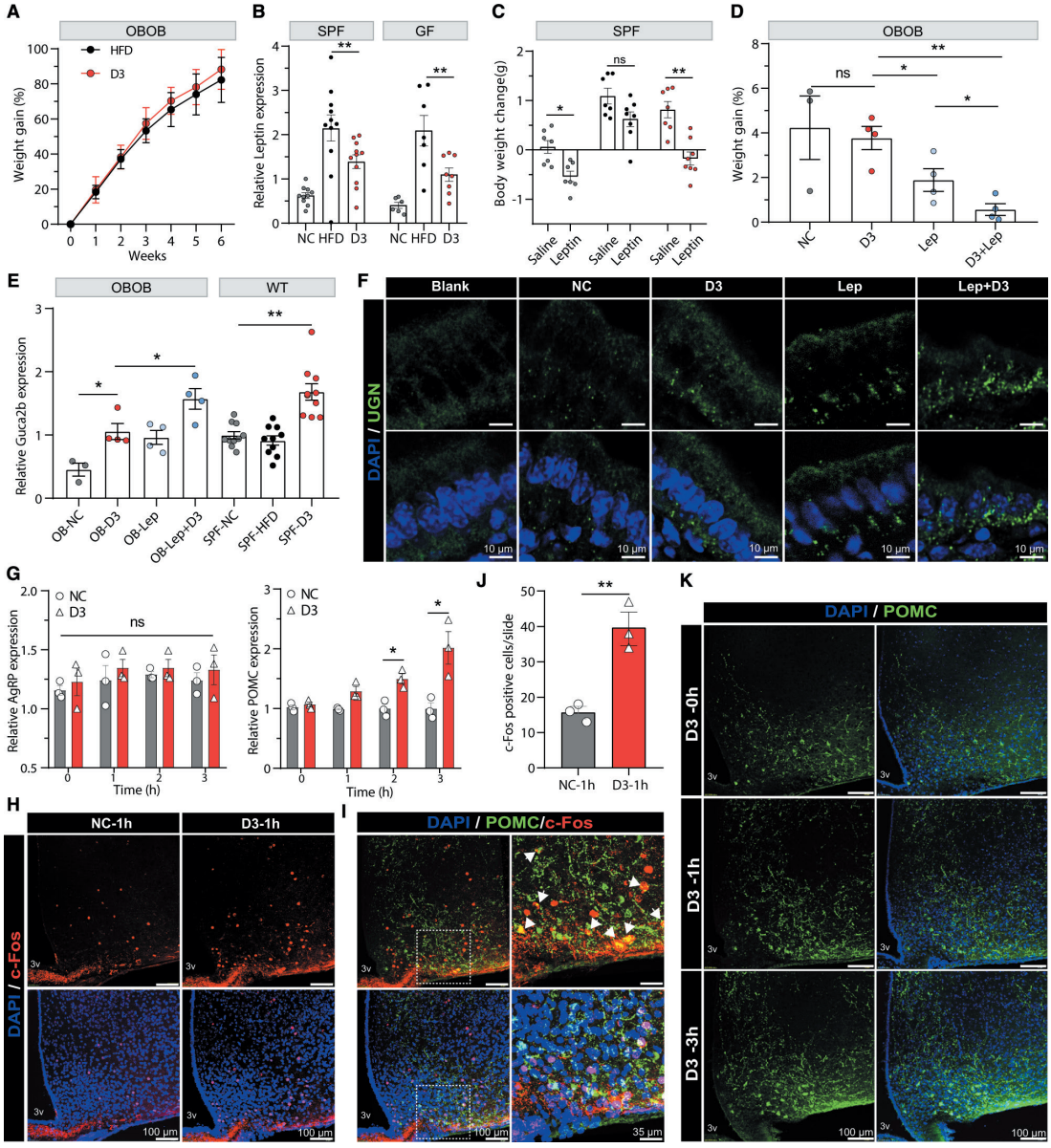

Figure 3 D3 increases leptin sensitivity and ARC c-Fos expression in mice. (A) Percentage of weight gain measured over time (ob/ob mice, n=8 per group). (B) Leptin mRNA expression levels of epididymis fat in specific pathogen-free/germ-free (SPF/GF) mice gavaged with D3 or saline as controls fed a high-fat-diet (HFD) or normal chow (NC) diet (SPF mice, n=10–12; GF mice, n=6–8). (C) Body weight change after treatment with exogenous leptin or saline (wild-type (WT) mice, n=7–8). Lute diagrams of the same colour represent two equally divided groups of mice with the same treatment. (D) Percentage of weight gain in ob/ob mice on normal diet with different treatments (NC, n=3; D3, leptin and D3+leptin, n=4). (E) Guca2b mRNA expression levels in ob/ob or WT mice (ob/ob mice, n=3–4 per group; WT mice n=8–10 per group). (F) Double immunofluorescence in ileal sections for uroguanylin (UGN) (green dots located at the base of intestinal epithelial cells) and nuclei (blue). Scale bars: 10 µm. (G) AgRp and POMC mRNA expression levels in WT mice (n=3 per group). (H) Representative images showing ARC c-FOS (red) and POMC (green) in SPF mice. Scale bar: 100 µm; 3v, the third cerebral ventricle. (I) Colocalisation of c-Fos positive cells with POMC neurons. (J) Numbers of c-Fos positive cells/slide in ARC of mice. (K) Double immunofluorescence in ARC sections for POMC (green) and nuclei (blue). Scale bars: 100 µm; 3v, the third cerebral ventricle. For A–E, H and J, p values were determined by a two-tailed Wilcoxon test, and data are presented as the means±SEM; *p<0.05; **p<0.01; ***p<0.001.

signals satiety and reduces food intake, to achieve the effect of appetite suppression.

D3 treatment increases the abundance of *A. muciniphila* in the gut microbiota

The gut microbiota is an important contributor to metabolic function and has been linked with the development of human diseases,[33 34] such as infantile autism[35] and obesity.[36] We next examined whether D3 protection against obesity was correlated with gut microbiota alteration. There was an obvious difference in the faecal microbiota composition between D3-treated and vehicle-treated mice (figure 4A,B and online supplemental figure 5a-c). The linear discriminant analysis showed that *Oscillospira*, *Lawsonia* and *Desulfovibrio* were significantly enriched in the vehicle-treated mice, whereas the genera *Bacteroides*, *Bilophila* and *Akkermansia* were significantly enriched in the D3-treated group (figure 4C).

Faecal microbiota transplantation (FMT), which entails the transfer of gut microbial communities from healthy donors to patients, has emerged as a promising treatment option for

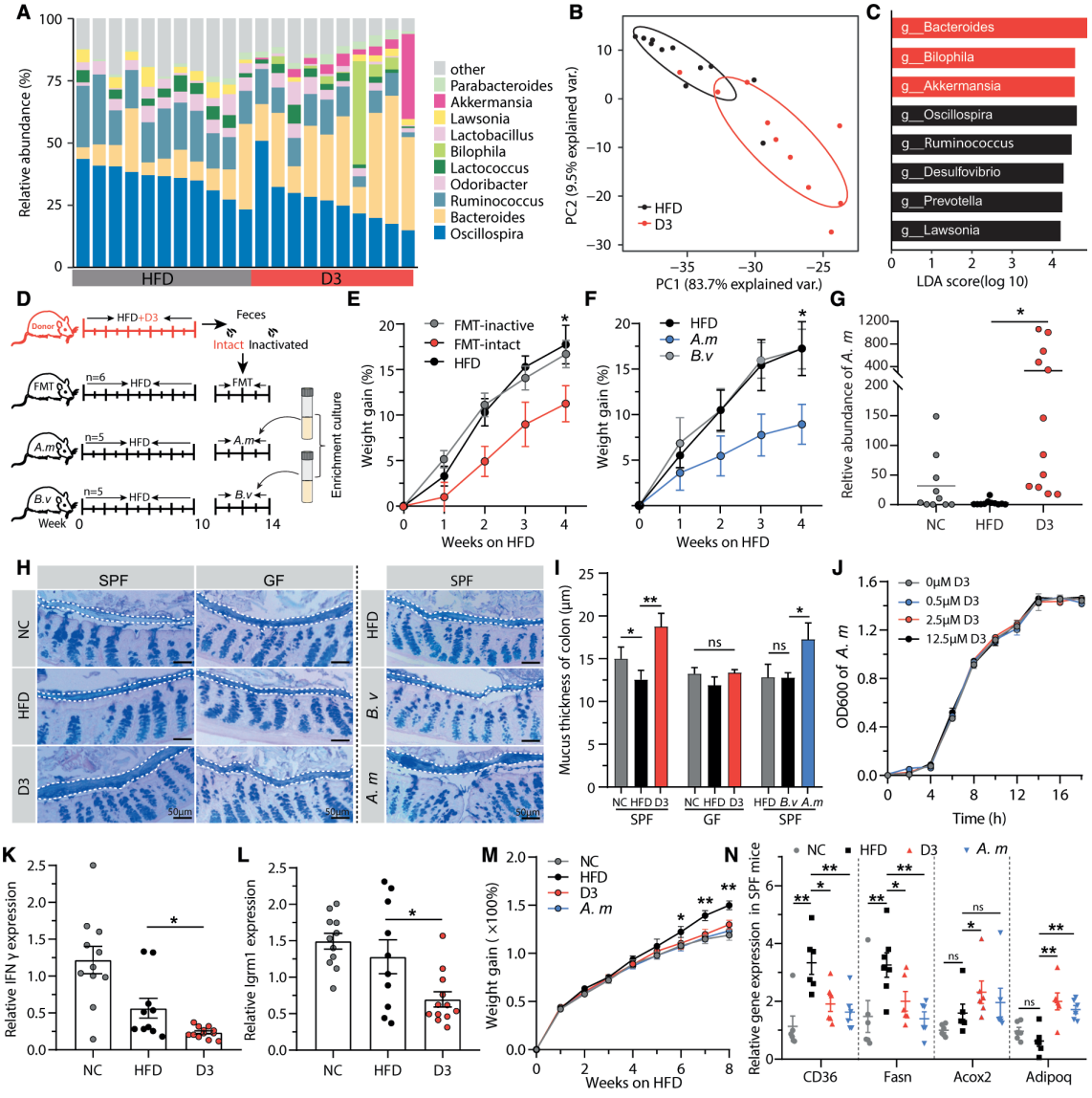

Figure 4 D3 alters the gut microbiota in mice. (A) Faecal microbiota composition in high-fat-diet (HFD)-treated and D3-treated mice at the genus level. (B) Principal component analysis (PCoA) of faecal microbiota in HFD and D3 mice. The significance of two separated clusters was measured with the Adonis test. (C) LEfSe analysis showing bacterial taxa that were significantly different in abundance between HFD and D3. Taxa significantly enriched and depleted in D3-treated mice are shown in red and black, respectively. (D) Experimental workflow of faecal microbiota transplantation (FMT). Mice were first fed an HFD for 10 weeks to achieve dietary obesity. During the next 4 weeks, D3-treated mice were used as the donors. Their faeces were collected and then divided into an inactivated group and an active group and eventually transferred to receptor mice via FMT. In addition, mice in the "*A. m*" and "*B. v*" *groups* were orally gavaged with 1×10^9 CFU of *Akkermansia muciniphila* or *Bacteroides vulgatus*. Donor and receptor, n=6 per group, "*A. m*" and "*B. v*" *group*, n=5 per group. (E–F) Percentage of weight gain measured over time (E, FMT; F, colonisation of exogenous bacteria), starting at the 14th week. (G) Relative abundance of *A. muciniphila* in the faecal samples of mice in figure 1D determined by quantitative PCR. (H–I) Periodic acid Schiff (PAS) and Alcian blue (AB) staining (H) and the thickness of the mucus layer (I) of colon sections from specific pathogen-free (SPF) and germ-free (GF) mice (figure 1D), as well as mice colonised by exogenous bacteria. The white dotted lines represent the boundaries of the mucus layer. (J) The growth curve of *A. muciniphila* exposed to different concentrations of D3 in vitro. Representative of three independent experiments. (K–I) IFNγ (K) and irgm1 (L) mRNA expression levels in ilea from SPF mice in figure 1D, Percentage of weight gain measured over time (n=6 mice per group). (N) CD36, Fasn and Acox2 (liver) and Adipoq (epididymis) mRNA expression levels of SPF mice fed a control diet (NC and HFD) or treated with D3 or gavaged with *A. muciniphila* (n = 6 mice per group). For E–G, I, and K–N, p values were determined by a two-tailed Wilcoxon test, and data are presented as the means±SEM; **p<0.01; ***p<0.001.

a range of chronic disorders.[37] Considering that compositional shifts in the gut microbiota may play a role during D3 treatment, we adopted FMT to determine whether the gut microbiota contributed to the rescue of obesity. The faecal microbiota from mice treated with D3 for 10 weeks were collected and orally given to the DIO mice. After 4 weeks, FMT promoted a 6.50%±2.91% weight reduction in the recipient mice compared with the HFD control mice, whereas the heat-inactivated faecal sample showed no effect (figure 4D,E). We wondered whether any particular faecal bacterial species exerted such protective effects. Therefore, we used two significantly enriched taxa (*B. vulgatus* and *A. muciniphila*) in the D3-treated DIO mice for 4 weeks. The colonisation of *A. muciniphila* led to a significant body weight reduction (p<0.05, Wilcoxon test), while the

colonisation of *B. vulgatus* did not have such an effect ($p>0.05$, Wilcoxon test) (figure 4F). This finding suggests that individual members (eg, *A. muciniphila*) of the gut microbiota transferred to recipient mice may defer obesity development in DIO mice, which is in agreement with previous studies.[38] We then returned to the initial experiment on the SPF mice and found that the abundance of *A. muciniphila* in the faeces of mice treated with D3 was approximately 100-fold higher than that in the HFD mice (figure 4G).

Recently, *A. muciniphila* was identified as a mucin-degrading bacterium that resides in the mucus layer.[39] The specialisation of *A. muciniphila* in mucin degradation makes it a key player at the mucosal interface between the lumen and host cells. By staining the mucus of the colonic epithelium, we found that the thickness of the mucus layer was significantly decreased in the HFD-fed mice (SPF). Both D3 and *A. muciniphila* treatment counteracted this decrease ($p<0.05$, Wilcoxon test). Interestingly, this effect disappeared when using D3 to treat GF mice (figure 4H,I). Therefore, we speculate that the thickening of the mucus layer is due to the colonisation of *A. muciniphila* rather than the direct action of D3.

To further explore the mechanism for the increase in the abundance of *A. muciniphila* that occurs with D3 treatment, we first measured the growth curve of *A. muciniphila* associated with exposure to different concentrations of D3 in vitro. As shown in figure 4J, there was no significant change under different D3 concentrations, indicating that D3 cannot promote the growth of *A. muciniphila* in vitro. Previous studies found that *A. muciniphila* was significantly increased in IFNγ-deficient mice, and the restoration of IFNγ levels could reduce *A. muciniphila* abundance.[40] IFNγ can induce the secretion of antimicrobial proteins from Paneth cells through Irgm1, a downstream molecule in its signalling cascade. Previous studies suggest that impaired production of antimicrobial peptides can lead to the overgrowth of *A. muciniphila* when the level of IFN or Irgm1 is reduced. In this study, we observed that D3 treatment significantly suppressed the expression of both IFNγ and Irgm1 in the ileum of mice relative to the HFD group (figure 4K,L). Therefore, we speculate that the increased abundance of *A. muciniphila* by D3 treatment may be attributed to the negative regulation of the IFNγ-Irgm1 axis.

To investigate whether *A. muciniphila* contributed to improving the phenotype of obese, we transplanted *A. muciniphila* into DIO mice for 8 weeks. Notably, *A. muciniphila* gavage with 1×10^9 CFU/mouse every 2 days led to a significant reduction ($p<0.01$, Wilcoxon test) in the body weight of mice, similar to the D3 treatment (figure 4M). We further compared the effects of *A. muciniphila* and D3 on lipid metabolism in DIO mice. We observed an increase in the expression of the Fasn and CD36 mRNAs, genes that regulate the synthesis and absorption of lipids,[41] a decrease in the mRNA level of Adipoq that promotes lipid oxidation in epididymal fat, after the administration of D3 or *A. muciniphila* in the SPF mice but not in GF mice (online supplemental figure 5f), suggesting additional positive effects of the increased *A. muciniphila*. Interestingly, a dramatic upregulation of Acox2, which can increase fatty acid oxidation and further inhibit lipid accumulation in the liver, was observed only in D3-treated SPF mice (figure 4N and online supplemental figure 5f).[42] These results indicate that the regulation of lipid metabolism should be a combined effect of D3 and *A. muciniphila*.

Recent studies showed that *A. muciniphila* could repair the thinning of the intestinal mucus caused by high-fat (HF) diet. Therefore, we further investigated how the administration of D3 or *A. muciniphila* affects the mucus in the colon. We found that the expression levels of MUC2 and IL4 were significantly increased after the administration of D3 or *A. muciniphila* in SPF mice ($p<0.05$, Wilcoxon test), but not in other markers of goblet cell development,[43] such as Klf4 ($p>0.05$, Wilcoxon test) (online supplemental figure 5d-e). However, GF mice treated by D3 did not show the same results, suggesting that the thickening of the mucus layer may be attributed to the increased abundance of *A. muciniphila* rather than the direct action of D3.

The anti-obesity effect of D3 in other animal models

To investigate the anti-obesity effect of D3 in other animals, we further treated two additional DIO models, rats and macaques, with D3 (figure 5A,H). Notably, D3 treatment resulted in an 8.96%±3.11% decrease in body weight gain in rats compared with untreated controls over the 10 weeks of HFD exposure ($p<0.05$, Wilcoxon test) (figure 5B,C,I). As expected, we observed that D3 treatment significantly suppressed food intake in DIO rats compared with HFD control rats ($p<0.05$, Wilcoxon test) (figure 5D). The expression of Guca2b in the ileum was significantly increased ($p<0.05$, Wilcoxon test) and leptin in epididymal fat was significantly decreased ($p<0.05$, Wilcoxon test) (figure 5E,F). Similarly, the abundance of *A. muciniphila* was increased ($p<0.05$, Wilcoxon test) (figure 5G). For DIO macaques, the average increase in body weight gain in the D3 group was 7.71%±2.97% lower than that in the control group at the 6th week (figure 5j). (figure 5I). Moreover, we observed that the food intake of macaques in the D3 group was significantly decreased ($p<0.05$, Wilcoxon test) (figure 5J), with an increased abundance of *A. muciniphila* ($p<0.05$, Wilcoxon test) (figure 5K).

DISCUSSION

Although obesity management has improved significantly over the years, therapies that target its underlying processes are still lacking. There is a growing interest in drug therapies that can support weight loss.[44] Currently, some endogenous peptides in humans have been used to treat type 2 diabetes and obesity, such as a K-casein-derived glycogenous peptide and casein.[45] Moreover, some intestinal peptides (eg, α-defensin 5) were used to reverse dyslipidaemia and improve glucoregulatory capacity in DIO mice.[21] We found that oral administration of D3 led to a 12.06%±2.35% decrease in body weight gain and ameliorated gut microbiota dysbiosis in DIO mice. We further demonstrated that D3 can upregulate the expression of UGN and leptin resistance, both of which can inhibit the appetite of mice. Our study provides a novel perspective and evidence that endogenous polypeptides derived from degraded fragments of protein precursors may play an important role in regulating obesity and other metabolic diseases (figure 5l).

To date, five medications (orlistat, phentermine plus topiramate, naltrexone plus bupropion, liraglutide and semaglutide), all of which have an anorexigenic effect, have been approved by the Food and Drug Administration (FDA) for long-term weight management in adults.[46] In this study, we found that after D3 treatment, the food intake of both SPF mice and GF mice was significantly reduced, accompanied by an increased expression of UGN in the small intestine. UGN, a 16-amino-acid anorexic hormone secreted by enterochromaffin cells in the small intestine, has been shown to target the GUCY2C receptor of the hypothalamus and activate anorexigenic pathways through blood circulation.[47] Intravenous injection of prouroguanylin could induce satiation in mice.[47] Kim *et al*[48] also found that transgenic UGN under a control of brain-specific promoter could produce

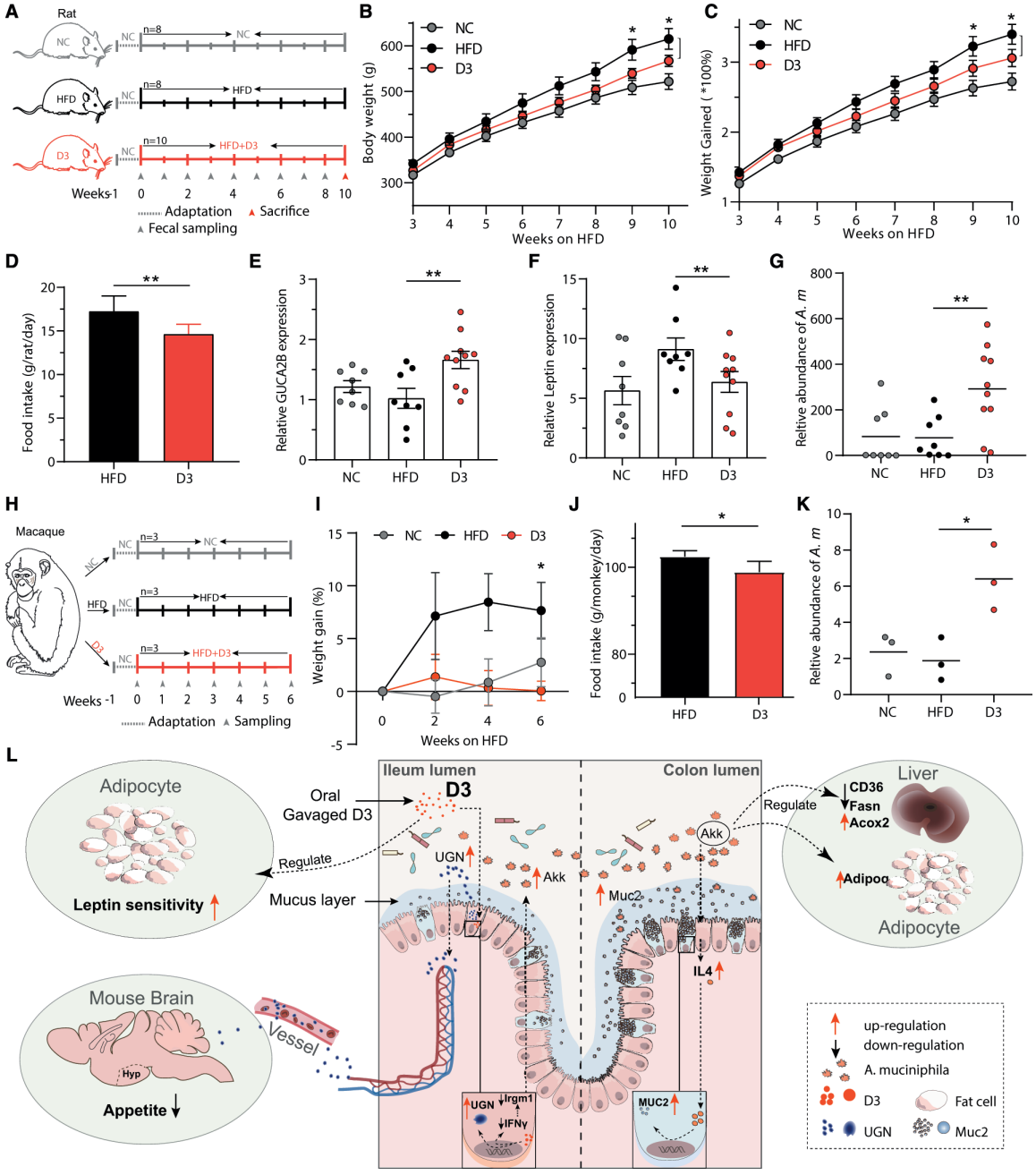

Figure 5 D3 protects rats and macaques from dietary obesity. (A) Experimental workflow in rats (n=8–10 per group). (B) Grams of weight gain of rats measured over time. (C) Percentage of weight gain of rats measured over time. The bracket represents a comparison between high-fat diet (HFD) and D3. (D) Food intake in rats measured every other day for 1 week. (E) Guca2b mRNA expression levels in the ileum of rats. (F) Leptin mRNA expression levels of epididymal fat in rats. (G) Relative abundance of *Akkermansia muciniphila* in the faecal samples of rats. (H) Experimental workflow in macaques fed a standard diet (normal chow, NC) or a HFD for 6 weeks (n=3 per group). (I) Percentage of weight gain of macaques measured over time. The bracket represents a comparison between HFD and D3. (J) Food intake in macaques measured every other day for 1 week. (K) Relative abundance of *A. muciniphila* in the faecal samples of macaques. (L) Summary of the role of D3 in treating obesity. As a leptin sensitiser, D3 can upregulate the expression of uroguanylin (UGN) in the ileum and suppress appetite by targeting the hypothalamus. D3 can also increase the abundance of *A. muciniphila* in the intestines, which in turn may influence lipid absorption and metabolism within the liver. For B–G and I–K, p values were determined by a two-tailed Wilcoxon test, and data are presented as the means±SEM; *p<0.05; **p<0.01.

physiological levels to induce durable anorexigenic responses opposing weight gain for at least 24 weeks without altering the metabolic rate in DIO mice. We found that D3 treatment could resist the onset and worsening of diet-induced obesity in mice by upregulating the expression of UGN and increasing its content in serum. Such a UGN (gut)-GUCY2C (hypothalamus) endocrine axis may have the potential to serve as a novel therapeutic target for appetite control and metabolic syndrome. Additionally, we found that D3 restored the compensatory leptin elevation caused by a HF diet and increased leptin sensitivity. Leptin can decrease appetite by inhibiting the activity of neurons in the ARC, the centre of appetite regulation in the hypothalamus.[49] A dramatic induction of c-Fos expression occurs when neurons in the ARC are activated by starvation, which can be reversed

by the administration of appetite inhibitors (eg, estradiol[50] and leptin[51]) or feeding.[32] Notably, the upregulated c-Fos expression and its colocalisation with POMC expressing neurons in mice after D3 administration, probably due to the combined effect of D3 promoting UGN expression and acting as a leptin sensitiser.

Currently, there is accumulating evidence of the role of gut microbiota in various metabolic disorders, and the manipulation of the gut microbiota might be a novel therapeutic option.[52 53] In our study, we found that D3 treatment could reduce the abundance of *Desulfovibrio* and *Ruminococcus*. The administration of *Desulfovibrio* to GF mice led to an increase in body fat percentage and the expression of CD36,[41] a critical regulator of lipid absorption and homeostasis within mammals.[54] In addition, we observed a higher abundance of *Bacteroides* in D3-treated mice. Many observational and interventional studies have correlated leanness or weight loss to increased levels of *Bacteroidetes*, which can produce short-chain fatty acids.[55] However, this relationship is controversial because observational studies have also found increased abundances of *Bacteroides* to be associated with Western diets, which are related to obesity.[56] Here, we found that significantly enriched colonisation with the taxon *B. vulgatus* for 4 weeks did not lead to a significant change in the body weight of DIO mice. In contrast, the obesity phenotype was reversed by transplanting *A. muciniphila* in obese mice, which is consistent with previous studies.[38 57] Notably, the difference between the percentage of body weight lost in GF mice (9.14%±2.93%) and SPF mice (12.06%±2.35%) treated with D3 further demonstrates the role of the gut microbiota in treating obesity. In fact, many drugs and chemicals that have been found to reduce body weight can affect the gut microbiota. For example, liraglutide changed the overall composition as well as the relative abundance of weight-relevant phylotypes, such as a reduction in *Proteobacteria* and an increase in *A. muciniphila* in treated DIO mice.[58] Interestingly, D3 treatment increased the abundance of *A. muciniphila* by 100 times, and this effect was much stronger than that of the previous two drugs (three to five times).

A number of polypeptides have been used to act as signalling molecules in the regulation of the neuroendocrine system to prevent obesity, including liraglutide and semaglutide,[44] glucagon-like peptide-1 (GLP-1) agonists and adrenomedullin 2.[14] However, several reasons may explain the slow adoption of injectable GLP-1R agonists, including poor adherence of this patient population to injectable therapies and the general patient preference for oral medicines compared with injectable therapies.[59] Interestingly, it is worth noting that in our study, oral administration of D3 significantly reduced the body weight of mice, indicating the potential of D3 as an effective and preferred treatment option for obesity. The use of medications for obesity has been limited by safety concerns. Among the drugs currently approved by the FDA for clinical use in the treatment of obesity, it seems that most of them have side effects. For example, GLP-1 analogues have been demonstrated to cause side effects, including transient nausea, GLP-1RA-related or insulin 'gastrointestinal' side effects[60] acute pancreatitis,[61] vomiting and a loss of appetite, which limit the dosage. Notably, no obvious side effects of D3 were observed in our study in mice, rats or macaques. Considering that our experiment was conducted only for 10–12 weeks, a longer experimental period is needed for verification of the results.

In summary, we report herein a small peptide, D3, that is not a GLP-1 analogue, can inhibit the development of obesity by suppressing appetite and regulating the gut microbiota. This study adds new evidence that the UGN-GUCY2G axis is a potential therapeutic target for the development of anti-obesity drugs and supportive evidence that D3 is a competitive candidate for counteracting diet-induced obesity with a favourable safety profile. The potential pleiotropic roles of this peptide in humans still need to be addressed in future research.

METHODS

Rational optimisation of hydrophobic peptides from human defensin HD5

A hidden Markov model as implemented in TMHMM Server V.2.0 was used to evaluate the peptides' abilities to penetrate cell membranes. The peptide secondary structure was modelled using SWISS-MODEL[62] with human HD5 (1zmp) as the template. The amphipathic surface and the three-dimensional structures of D1-4 were modelled using PyMol V.2.3.2.[63] D1–4 were synthesised using solid phase synthesis by Mimotopes (Wuxi, China).

Bacterial strains and administration and faecal microbial transplantation

Bacteroides vulgatus ATCC 8248 and *Akkermansia muciniphila* (ATCC BAA-835) were grown anaerobically at 37°C in Gifu anaerobic medium (HB8518-1, Hopepiol, Qingdao). Mice were treated with *B. vulgatus* and *A. muciniphila* by oral gavage at a dose of 1×10^9 CFU/0.2 mL suspended in sterile anaerobic phosphate buffered saline (PBS). A similar concentration of glycerol (2.5% vol/vol) was used as control. Treatments were continued for 4 weeks.

For the FMT experiment, 2–3 fresh faecal pellets were resuspended by vortexing in anaerobic PBS, and then the supernatant was harvested and mixed. Bacteria were harvested and resuspended in sterile and anaerobic PBS before FMT, and 100 µL of the suspension was administered to the mice by oral gavage two times per day for 4 weeks. Additionally, inactivated bacteria treated with high temperature were also administered to the mice by oral gavage two times per day for 4 weeks, which served as a control.

Animals and experiments

Operation of SPF mice and rats

All C57/Bl6J mice and Sprague Dawley (SD) rats (SPF Biotechnology, Beijing, China) and ob/ob mice (Hua Fukang Biotechnology, Beijing, China) were housed in groups of 4–6 animals per cage in a pathogen-free facility with standard bedding and enrichment in a temperature-controlled and humidity-controlled room on a 12-hour light/dark cycle with free access to food and water. All animals were fed a standard laboratory chow diet (growth and reproduction diet, SPFSLFZ003, SPF Biotechnology, Beijing, China) unless otherwise stated. HFD mice or rats were fed a HF diet (Rodent diet with 60 kcal% fat, D12492; Research diets, New Brunswick, New Jersey, USA). For rats, only D3 was used. After 1 week of recovery, animals were randomly assigned to treatment groups, and treatment continued for 10 weeks. Food intake and body weight were monitored weekly. Fresh excreta from animals were harvested and stored at −80°C for further analysis. All of the above experiments in mice and rats were started at 4 weeks of age, unless otherwise noted.

Operation of GF mice

GF C57Bl/6 mice obtained from the Department of Laboratory Animal Science of the Army Medical University (Chongqing, China) were used. Mice and rats were sacrificed by cervical dislocation. Relevant organs were collected and immediately immersed in liquid nitrogen and stored at −80°C for further

analysis. Subcutaneous and visceral adipose deposits were precisely dissected and weighed.

Pair-feeding

The pair-feeding experiment was performed according to previously reported procedures.[64] Pair feeding was accomplished by measuring the food intake of the ad libitum-fed D3-treated mice every 24 hours and presenting this amount of food to the pair-fed PBS-treated mice in two times (half within 12 hours). Blood samples were obtained, and tissues were harvested as described above.

Operation of macaques

The rhesus experiment was undertaken by Beijing Prima Biotech. Nine rhesus monkeys feeding on a standard chow diet (#2150230401, Prima Biotech, Beijing, China) were randomly assigned to three treatment groups: D3, NC and HFD.

Short-term food intake measurement

Food weights were recorded every other day over a period of 1 week, and the average intake per day for each 2-day period was determined and averaged over the week measurement period for each individual.

Antibiotic treatment

SPF WT mice were treated with combined antibiotics (ABX) containing 100 g/L neomycin (Sigma), 100 g/L penicillin (Sigma), 50 g/L vancomycin (Sigma) and 100 g/L metronidazole (Sigma) for 8 weeks.

Morphology and histology

Liver and adipose tissue samples were quickly collected and fixed in 4% paraformaldehyde (PFA) solution for 24 hours and embedded in paraffin. Sections of 10 µm were stained with H&E. ABPAS staining was performed using a previous method.[65] A minimum of 10 different measurements were made perpendicular to the inner mucus layer per field and were manually delineated and analysed by ImageJ.

Localisation of D3 after oral administration

FITC-D3 is used to trace drugs in target organs and their action pathways. The Swiss rolls were made according to previously published methods,[65] with minor modifications. Briefly, after oral administration of 0.8 mg/kg FITC-D3 for 3 hours, the mice were sacrificed, and the lumen of small intestine was cut open from one side of the intestine using spring scissors. Cotton swabs were used to roll up the intestines that had been unfolded. The intestines were gently rolled around the self-closing forceps evenly, ensuring that each successive roll neatly laid over the previous roll with edges flush. The roll was gently slid off the cotton swabs and placed into an appropriately labelled pot containing 10 times the tissue volume of formalin. Whole-tissue slide scans at ×40 magnification were performed under a microscope slide scanner (Pannoramic MIDI, 3DHISTECH). Images were analysed with ZEN Imaging Software by ZEISS. Pictures were obtained by using an LSM 880 (Zeiss) or a spinning disc confocal microscope (Olympus).

For the localisation of D3 uptake in cells, HCT116 cells were inoculated into confocal dishes (1×10^5 cells/well) and incubated for 18 hours at 37°C. Free FITC (10 µM) or FITC-labelled D3 (10 µM) was added to cultures for 1 hour. Following staining, the cells were washed twice with PBS and later observed under a spinning disc confocal microscope (Olympus) after the addition of fresh medium.

Immunofluorescence of the ileum and hypothalamus

Tissue segments were immediately removed, washed with PBS, mounted in embedding medium (Tissue-Te, O.C.T. Compound) and stored (−80°C) until use. Immunofluorescence was performed using an anti-UGN (1:200; MBS7605526; MyBioSource) antibody. Detection and labelling were performed with secondary antibodies conjugated to Alexa Fluor-488 donkey anti-rabbit IgG (H+L) (1/500, A21206, Invitrogen).

Neuronal identification and c-Fos staining

Twenty-four mice (male, 8 weeks old) feeding on a standard chow diet were equally divided into eight groups (NC-0h, NC-1h, NC-2h, NC-3h; D3-0h, D3-1h, D3-2h, D3-3h). For gene expression assays, the hypothalamus was harvested 0–3 hours following D3 administration (NC: saline), and the expression levels of c-Fos, AgRp and Pomc were quantified by quantitative RT-PCR.

The same experiment was carried out for the immunofluorescence. c-Fos staining was performed as described in a previous study.[66] Briefly, mice were anaesthetised with a lethal dose of pentobarbital and transcardially perfused with PBS followed by 4% paraformaldehyde. Brains were removed, placed in 4% paraformaldehyde overnight and dehydrated in 30% sucrose for 1 week. Brains were cut into 25 mm sections. The sections were treated as described above and incubated overnight at room temperature in mouse anti-FOS (1:500; ab208942; Abcam) or rabbit anti-POMC (1:100; ab254257; Abcam). Detection and labelling were performed using secondary antibodies conjugated to Alexa Fluor-594 donkey anti-mouse IgG (H+L) (1/500, ab150108, Abcam) or Alexa Fluor-488 donkey anti-rabbit IgG (H+L) (1/500, ab150073, Abcam), and imaging was performed as described above. Images were pseudocoloured using Photoshop software (Adobe) or ImageJ (NIH).

Twitter Fangqing Zhao @Fangqing_Zhao

Contributors FZ is responsible for the overall content as the guarantor. FZ conceived and supervised the study. FZ and ZL designed the study, interpreted the results and wrote the manuscript. WH's team fed the GF mice and recorded the experimental data. Ileal transcriptome and faecal flora diversity analyses were performed by BZ. ZL, HW, ZZ and NW performed all the other experiments and the data analysis and prepared the figures and tables.

Funding This work was supported by grants from the National Natural Science Foundation of China (32025009, 32001082), National Key R&D Project (2021YFA1301000, 2021YFC2301300) and the Strategic Priority Research Program of Chinese Academy of Sciences (XDB38020300). We thank Jingwei Wang, Xiuling Ma, You Yu and Yongxi Huang for their assistance in sample preprocessing.

Competing interests None declared.

Patient consent for publication Not applicable.

Ethics approval All animal studies were approved by the Institutional Animal Care and Use Committee of Institute of Zoology, Chinese Academy of Sciences (IOZ-IACUC-2020–091).

Provenance and peer review Not commissioned; externally peer reviewed.

Data availability statement Data are available upon reasonable request.

ORCID iD
Fangqing Zhao http://orcid.org/0000-0002-6216-1235

REFERENCES

1 van Son J, Koekkoek LL, La Fleur SE, *et al*. The role of the gut microbiota in the gut-brain axis in obesity: mechanisms and future implications. *Int J Mol Sci* 2021;22. doi:10.3390/ijms22062993. [Epub ahead of print: 15 Mar 2021].
2 Heymsfield SB, Wadden TA. Mechanisms, pathophysiology, and management of obesity. *N Engl J Med* 2017;376:254–66.
3 Yeh T-L, Chen H-H, Chiu H-H, *et al*. Morbidity associated with overweight and obesity in health personnel: a 10-year retrospective of hospital-based cohort study in Taiwan. *Diabetes Metab Syndr Obes* 2019;12:267–74.
4 Ramos Salas X, Salas XR. The ineffectiveness and unintended consequences of the public health war on obesity. *Can J Public Health* 2015;106:E79.
5 Schéle E, Grahnemo L, Anesten F, *et al*. The gut microbiota reduces leptin sensitivity and the expression of the obesity-suppressing neuropeptides proglucagon (GCG) and brain-derived neurotrophic factor (BDNF) in the central nervous system. *Endocrinology* 2013;154:3643–51.
6 Bäckhed F, Ding H, Wang T, *et al*. The gut microbiota as an environmental factor that regulates fat storage. *Proc Natl Acad Sci U S A* 2004;101:15718–23.
7 Cani PD, Cani, Patrice D. Human gut microbiome: hopes, threats and promises. *Gut* 2018;67:1716–25.
8 Li F, Jiang C, Krausz KW, *et al*. Microbiome remodelling leads to inhibition of intestinal farnesoid X receptor signalling and decreased obesity. *Nat Commun* 2013;4:2384.
9 Anhê FF, Roy D, Pilon G, *et al*. A polyphenol-rich cranberry extract protects from diet-induced obesity, insulin resistance and intestinal inflammation in association with increased Akkermansia spp. population in the gut microbiota of mice. *Gut* 2015;64:872–83.
10 Shin N-R, Lee J-C, Lee H-Y, *et al*. An increase in the Akkermansia spp. population induced by metformin treatment improves glucose homeostasis in diet-induced obese mice. *Gut* 2014;63:727–35.
11 Org E, Mehrabian M, Lusis AJ. Unraveling the environmental and genetic interactions in atherosclerosis: Central role of the gut microbiota. *Atherosclerosis* 2015;241:387–99.
12 Liu R, Hong J, Xu X, *et al*. Gut microbiome and serum metabolome alterations in obesity and after weight-loss intervention. *Nat Med* 2017;23:859–68.
13 Cheng Y-C, Liu J-R. Effect of *Lactobacillus rhamnosus* GG on Energy Metabolism, Leptin Resistance, and Gut Microbiota in Mice with Diet-Induced Obesity. *Nutrients* 2020;12. doi:10.3390/nu12092557. [Epub ahead of print: 24 Aug 2020].
14 Fosgerau K, Hoffmann T. Peptide therapeutics: current status and future directions. *Drug Discov Today* 2015;20:122–8.
15 Xu F, Lin B, Zheng X, *et al*. GLP-1 receptor agonist promotes brown remodelling in mouse white adipose tissue through SIRT1. *Diabetologia* 2016;59:1059–69.
16 Bordicchia M, Liu D, Amri E-Z, *et al*. Cardiac natriuretic peptides act via p38 MAPK to induce the brown fat thermogenic program in mouse and human adipocytes. *J Clin Invest* 2012;122:1022–36.
17 Fournel A, Drougard A, Duparc T, *et al*. Apelin targets gut contraction to control glucose metabolism via the brain. *Gut* 2017;66:258–69.
18 Abbasi J. Semaglutide's Success Could Usher in a "New Dawn" for Obesity Treatment. *JAMA* 2021.
19 Sun L. Peptide-based drug development. *Mod Chem Appl* 2013;01:1–2.
20 Omarova M, Zhang Y, Mkam Tsengam IK, *et al*. Hydrophobe containing Polypeptoids complex with lipids and induce Fusogenesis of lipid vesicles. *J Phys Chem B* 2021;125:3145–52.
21 Larsen IS, Fritzen AM, Carl CS, *et al*. Human Paneth cell α-defensin-5 treatment reverses dyslipidemia and improves glucoregulatory capacity in diet-induced obese mice. *Am J Physiol Endocrinol Metab* 2019;317:E42–52.
22 Ehmann D, Wendler J, Koeninger L, *et al*. Paneth cell α-defensins HD-5 and HD-6 display differential degradation into active antimicrobial fragments. *Proc Natl Acad Sci U S A* 2019;116:3746–51.
23 Fischer R, Fotin-Mleczek M, Hufnagel H. Break on through to the other side-biophysics and cell biology shed light on cell-penetrating peptides. *Chembiochem* 2010;6.
24 Mikkelsen TS, Xu Z, Zhang X, *et al*. Comparative epigenomic analysis of murine and human adipogenesis. *Cell* 2010;143:156–69.
25 Lazra Y, Falach A, Frenkel L, *et al*. Autocrine/paracrine function of globular adiponectin: inhibition of lipid metabolism and inflammatory response in 3T3-L1 adipocytes. *J Cell Biochem* 2015;116:754–66.
26 Moore MJ, Blachere NE, Fak JJ, *et al*. ZFP36 RNA-binding proteins restrain T cell activation and anti-viral immunity. *Elife* 2018;7. doi:10.7554/eLife.33057. [Epub ahead of print: 31 05 2018].
27 Folgueira C, Barja-Fernandez S, Gonzalez-Saenz P, *et al*. Uroguanylin: a new actor in the energy balance movie. *J Mol Endocrinol* 2018;60:R31–8.
28 Izquierdo AG, Crujeiras AB, Casanueva FF, *et al*. Leptin, obesity, and leptin resistance: where are we 25 years later? *Nutrients* 2019;11. doi:10.3390/nu11112704. [Epub ahead of print: 08 Nov 2019].
29 Münzberg H, Flier JS, Bjørbaek C. Region-specific leptin resistance within the hypothalamus of diet-induced obese mice. *Endocrinology* 2004;145:4880–9.
30 Lubis AR, Widia F, Soegondo S, *et al*. The role of SOCS-3 protein in leptin resistance and obesity. *Acta Med Indones* 2008;40:89–95.
31 Folgueira C, Beiroa D, González-Rellán MJ, *et al*. Uroguanylin improves leptin responsiveness in diet-induced obese mice. *Nutrients* 2019;11. doi:10.3390/nu11040752. [Epub ahead of print: 30 Mar 2019].
32 Munzberg H, Jobst EE, Bates SH, *et al*. Appropriate inhibition of orexigenic hypothalamic arcuate nucleus neurons independently of leptin Receptor/STAT3 signaling. *J Neurosci* 2007;27:69–74.
33 Wang J, Zheng J, Shi W, *et al*. Dysbiosis of maternal and neonatal microbiota associated with gestational diabetes mellitus. *Gut* 2018;67:1614–25.
34 Xiao L, Wang J, Zheng J, *et al*. Deterministic transition of enterotypes shapes the infant gut microbiome at an early age. *Genome Biol* 2021;22:243.
35 Yu Y, Zhang B, Ji P, *et al*. Changes to gut amino acid transporters and microbiome associated with increased E/I ratio in Chd8$^{+/-}$ mouse model of ASD-like behavior. *Nat Commun* 2022;13:1151.
36 Ussar S, Griffin NW, Bezy O, *et al*. Interactions between gut microbiota, host genetics and diet modulate the predisposition to obesity and metabolic syndrome. *Cell Metab* 2015;22:516–30.
37 Li SS, Zhu A, Benes V, *et al*. Durable coexistence of donor and recipient strains after fecal microbiota transplantation. *Science* 2016;352:586–9.
38 Dao MC, Everard A, Aron-Wisnewsky J, *et al*. Akkermansia muciniphila and improved metabolic health during a dietary intervention in obesity: relationship with gut microbiome richness and ecology. *Gut* 2016;65:426–36.
39 Derrien M, Vaughan EE, Plugge CM, *et al*. Akkermansia muciniphila gen. nov., sp. nov., a human intestinal mucin-degrading bacterium. *Int J Syst Evol Microbiol* 2004;54:1469–76.
40 Greer RL, Dong X, Moraes ACF, *et al*. Akkermansia muciniphila mediates negative effects of IFNγ on glucose metabolism. *Nat Commun* 2016;7:13329.
41 Petersen C, Bell R, Klag KA, *et al*. T cell-mediated regulation of the microbiota protects against obesity. *Science* 2019;365. doi:10.1126/science.aat9351. [Epub ahead of print: 26 07 2019].
42 Sharma RS, Harrison DJ, Kisielewski D, *et al*. Experimental Nonalcoholic Steatohepatitis and Liver Fibrosis Are Ameliorated by Pharmacologic Activation of Nrf2 (NF-E2 p45-Related Factor 2). *Cell Mol Gastroenterol Hepatol* 2018;5:367–98.
43 Waddell A, Vallance JE, Hummel A, *et al*. Il-33 induces murine intestinal goblet cell differentiation indirectly via innate lymphoid cell IL-13 secretion. *J Immunol* 2019;202:598–607.
44 Williams DM, Nawaz A, Evans M. Drug therapy in obesity: a review of current and emerging treatments. *Diabetes Ther* 2020;11:1199–216.
45 Cui X, Li Y, Yang L, *et al*. Peptidome analysis of human milk from women delivering macrosomic fetuses reveals multiple means of protection for infants. *Oncotarget* 2016;7:63514–25.
46 Yanovski SZ, Yanovski JA. Progress in pharmacotherapy for obesity. *JAMA* 2021;326:129.
47 Valentino MA, Lin JE, Snook AE, *et al*. A uroguanylin-GUCY2C endocrine axis regulates feeding in mice. *J Clin Invest* 2011;121:3578–88.
48 Kim GW, Lin JE, Snook AE, *et al*. Calorie-induced ER stress suppresses uroguanylin satiety signaling in diet-induced obesity. *Nutr Diabetes* 2016;6:e211.
49 Xu J, Bartolome CL, Low CS, *et al*. Genetic identification of leptin neural circuits in energy and glucose homeostases. *Nature* 2018;556:505–9.
50 Olofsson LE, Pierce AA, Xu AW. Functional requirement of AgRP and NPY neurons in ovarian cycle-dependent regulation of food intake. *Proc Natl Acad Sci U S A* 2009;106:15932–7.
51 Münzberg H, Jobst EE, Bates SH, *et al*. Appropriate inhibition of orexigenic hypothalamic arcuate nucleus neurons independently of leptin receptor/STAT3 signaling. *J Neurosci* 2007;27:69–74.
52 Turnbaugh PJ, Ley RE, Mahowald MA, *et al*. An obesity-associated gut microbiome with increased capacity for energy harvest. *Nature* 2006;444:1027–31.
53 Wang J, Li Z, Ma X, *et al*. Translocation of vaginal microbiota is involved in impairment and protection of uterine health. *Nat Commun* 2021;12:4191.
54 Buttet M, Traynard V, Tran TTT, *et al*. From fatty-acid sensing to chylomicron synthesis: role of intestinal lipid-binding proteins. *Biochimie* 2014;96:37–47.
55 Rios-Covian D, Salazar N, Gueimonde M, *et al*. Shaping the Metabolism of Intestinal *Bacteroides* Population through Diet to Improve Human Health. *Front Microbiol* 2017;8:376.
56 De Filippis F, Pellegrini N, Laghi L, *et al*. Unusual sub-genus associations of faecal Prevotella and Bacteroides with specific dietary patterns. *Microbiome* 2016;4:57.
57 Everard A, Belzer C, Geurts L, *et al*. Cross-talk between Akkermansia muciniphila and intestinal epithelium controls diet-induced obesity. *Proc Natl Acad Sci U S A* 2013;110:9066–71.
58 Moreira GV, Azevedo FF, Ribeiro LM, *et al*. Liraglutide modulates gut microbiota and reduces NAFLD in obese mice. *J Nutr Biochem* 2018;62:143–54.
59 Holko P, Kawalec P, Mossakowska M. Quality of life related to oral, subcutaneous, and intravenous biologic treatment of inflammatory bowel disease: a time trade-off study. *Eur J Gastroenterol Hepatol* 2018;30:174–80.
60 Shyangdan DS, Royle P, Clar C, *et al*. Glucagon-like peptide analogues for type 2 diabetes mellitus. *Cochrane Database Syst Rev* 2011:CD006423.

61 Nauck M. Incretin therapies: highlighting common features and differences in the modes of action of glucagon-like peptide-1 receptor agonists and dipeptidyl peptidase-4 inhibitors. *Diabetes, Obesity and Metabolism* 2016;18:203–16.
62 Waterhouse A, Bertoni M, Bienert S, *et al*. SWISS-MODEL: homology modelling of protein structures and complexes. *Nucleic Acids Res* 2018;46:W296–303.
63 Student G. The PyMOL molecular graphics system, version 1.5.0.1 Schrödinger, LLC. *CARBNews_Wall_systems_R30_and_beyond*.
64 Ellacott KLJ, Morton GJ, Woods SC, *et al*. Assessment of feeding behavior in laboratory mice. *Cell Metab* 2010;12:10–17.
65 Hansson GC, Johansson ME. The inner of the two MUC2 mucin-dependent mucus layers in colon is devoid of bacteria. *Gut Microbes* 2008;105:51–4.
66 Cheng W, Gonzalez I, Pan W, *et al*. Calcitonin receptor neurons in the mouse nucleus tractus solitarius control energy balance via the Non-aversive suppression of feeding. *Cell Metab* 2020;31:301–12.

Supplementary Materials for

A novel peptide protects against diet-induced obesity by suppressing appetite and modulating the gut microbiota

Methods

Cytotoxicity of D3

A Cell Titer Glo kit was used to measure the cytotoxicity of D3 on the viability of HCT116 cells according to the manufacturer's instructions. Briefly, HCT116 cells were seeded into a 384-well cell plate (1000 cells/well) and incubated overnight at 37 °C and 5% (v/v) CO_2. D3 at different concentrations was coincubated with cells for another 72 h at 37 °C and 5% (v/v) CO_2. Finally, the luminescence signal was recorded by an Envision microplate reader.

The hemolytic activity of D3 was evaluated by determining the amount of hemoglobin released from the blood cells. Mouse erythrocytes were collected and washed three times with PBS (pH 7.2) and then centrifuged at 1,500 rpm for 10 min. Then, 100 μl of erythrocyte solution (8%, v/v) was mixed with 100 μl of a series of peptide solutions and incubated for 1 h at 37 °C. The mixture was then centrifuged at 1,500 rpm for 5 min, and the absorbance of supernatants was measured at 540 nm. Values of 0 and 100% hemolysis were determined in PBS and 0.1% Triton X-100, respectively. Three replicates were performed for each condition. Hemolysis (%) = [Abs540 nm of the treated sample - Abs540 nm of the negative control)/(Abs540 nm of the positive control - Abs540 nm of the negative control)] × 100.

Leptin sensitivity measurement

The first assay is to determine the responses of body weight to leptin administration, which was performed according to the procedure proposed by Yu et al.[1, 2]. After 10 weeks of HFD or D3 treatment, the mice in each group were divided into two subgroups and received intraperitoneally administered leptin (1 μg/g body weight) or vehicle twice daily for 3 days. Recombinant murine leptin (ChinaPeptides Co., Ltd.) was dissolved in 0.9% NaCl solution and sterile filtered through a 0.22-μm

Li Z, *et al. Gut* 2022;0:1–13. doi: 10.1136/gutjnl-2022-328035

filter. Body weights were measured twice daily before and after the leptin injection.

The second assay is to detect the leptin-stimulated cytokines according to previous studies[3, 4]. After 8 weeks of HFD or D3 treatment, Mice were injected ip with leptin (5.0 mg/kg body weight) or vehicle (PBS) and anesthetized 25 min later, and the brains were immediately removed, frozen and stored at −80 °C. The mRNA of SOCS-3, PTP1B and PI3K was quantified by RT-PCR using RNA isolated from microdissected arcuate nucleus[5].

Indirect calorimetry

The metabolic parameters oxygen consumption (VO2) and carbon dioxide production (VCO2) were determined by an indirect calorimetry system (TSE Systems, Bad Homburg, Germany)[6]. Briefly, mice were acclimated in training cages for 3 days prior to the measurement and were allowed 4 additional days to acclimate to the TSE cabinets92. Gas exchanges were recorded every 20 minutes over 20 hours.

Glucose tolerance testing

After fasting for 6 h, mice were treated with oral gavage glucose (2 g/kg body weight)[7, 8] at 9:00 a.m. Blood samples were collected from the tip of the tail vein, and blood glucose was measured at 0 (immediately before glucose injection), 15, 30, 60 and 120 min with a Freestyle Lite glucose meter (Accu Check, Roche, Switzerland).

Insulin tolerance test (ITT)

Mice were intraperitoneally injected with insulin (1.0 U/kg body weight) at 9:00 a.m. Blood glucose levels were measured from the tail vein at 0, 15, 30, 60, 90, and 120 min as described above[7, 8].

DNA isolation, 16S rRNA sequencing and quantitative PCR

Bacterial DNA was extracted from the fecal samples using a QIAamp-DNA mini stool kit (QIAGEN, CA, USA). After 16S rRNA (V3-V4) amplicon sequencing, the abundance and diversity of intestinal flora in mice were determined using Illumina HiSeq sequencing (I-Sanger, Beijing, China). The QIIME software package was used to conduct the bioinformatic analyses of the sequences as described previously. Sequences with 97% sequence identity were attributed to the same operational taxonomic units (OTUs), and the OTU table was picked using the open reference

picking strategy based on the Greengenes database. Linear discriminant analysis (LDA) effect size (LEfSe) analysis was conducted to identify discriminatory bacteria, with an absolute value of the log LDA score >3.0 being considered a differential signature, which was significantly better in discriminating between different groups. QIME was used for principal coordinate analysis depending on the unweighted UniFrac distances, and intergroup comparisons were conducted using Wilcoxon rank-sum tests.

A. muciniphila was quantified with qPCR as described in Everard et al.[9]. Briefly, a total of 10 ng of DNA was used for quantitative PCR (qPCR). Primers for *A. muciniphila* (AM1: 5'-CAGCACGTGAAGGTGGGGAC-3', AM2: 5'-CCTTGCGGTTGGCTTCAGAT-3') and total bacteria (27F: 5'-AGAGTTTGATCCTGGCTCAG-3', 1492R: 5'-GGWTACCTTGTTACGACTT-3') and the relative abundance of target bacteria were calculated using the $2^{-\Delta\Delta Ct}$ method.

RNA extraction, and RT-qPCR, and RNA-seq data analysis

Total RNA was extracted from the ileum or fat tissue of animals using TRIzol reagent (Invitrogen, Carlsbad, CA) according to the manufacturer's instructions. cDNA was prepared by reverse transcription of 1-2 μg total RNA with reverse transcription enzyme (Yeasen, Shanghai, China). The target primers used are listed in Supplementary Table 2. qPCR detection was performed with the StepOnePlus real-time PCR system and software (Applied Biosystems, Foster City, USA). The results of gene expression are presented as a percentage expression of each gene normalized with glyceraldehyde-3-phosphate dehydrogenase (GAPDH) as a reference. RNA-seq data were first trimmed to remove low-quality bases using trim galore v0.4.4. HISAT2 v2.0.5 and StringTie v1.3.4[10] were used to quantify gene abundance with GRCm38 as the mouse reference genome. Differential expression (DE) analysis was performed using DESeq2 v1.24.0. Genes with significant DE were those with a 2-fold change cutoff and an adjusted P value < 0.05. Gene Ontology enrichment analysis (GOEA) was performed using the R package cluster Profiler v3.12.0. The results of GOEA were visualized in Goplot v1.0.2[11].

Supplementary figures

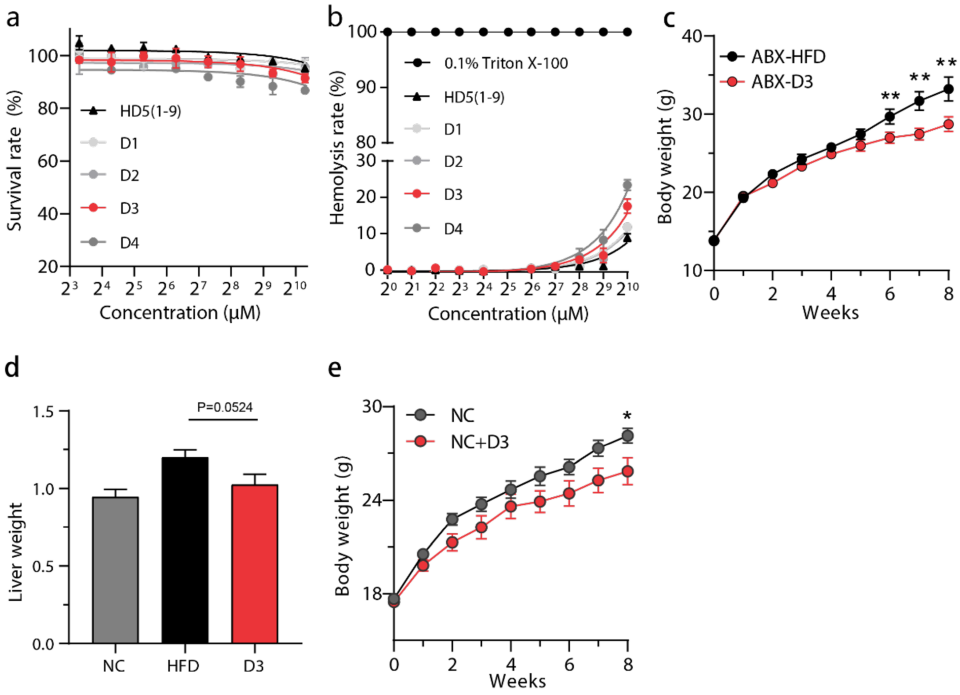

Supplementary Figure 1. Oral administration of D3 counteracts obesity. a, The cytotoxic activity of D1-4 to mouse Hct116 cells. The y-axis represents survival rate. **b**, Hemolytic activity of D1-4 against murine erythrocytes. **c**. Grams of weight gain measured over time, starting at 4 weeks of age (ABX: antibiotic mixture; n=6 per group). **d**, Total weight of liver. **e**. Grams of weight gain measured over time, starting at 4 weeks of age; (n=6 per group). For **a** and **b**, Deming regression was used to evaluate the trend in toxicity with different D3 concentrations. For **c-e**, *P* values were determined by a two-tailed Wilcoxon test, and data are presented as the means ± s.e.m; $P < 0.05$ (*); $P < 0.01$ (**).

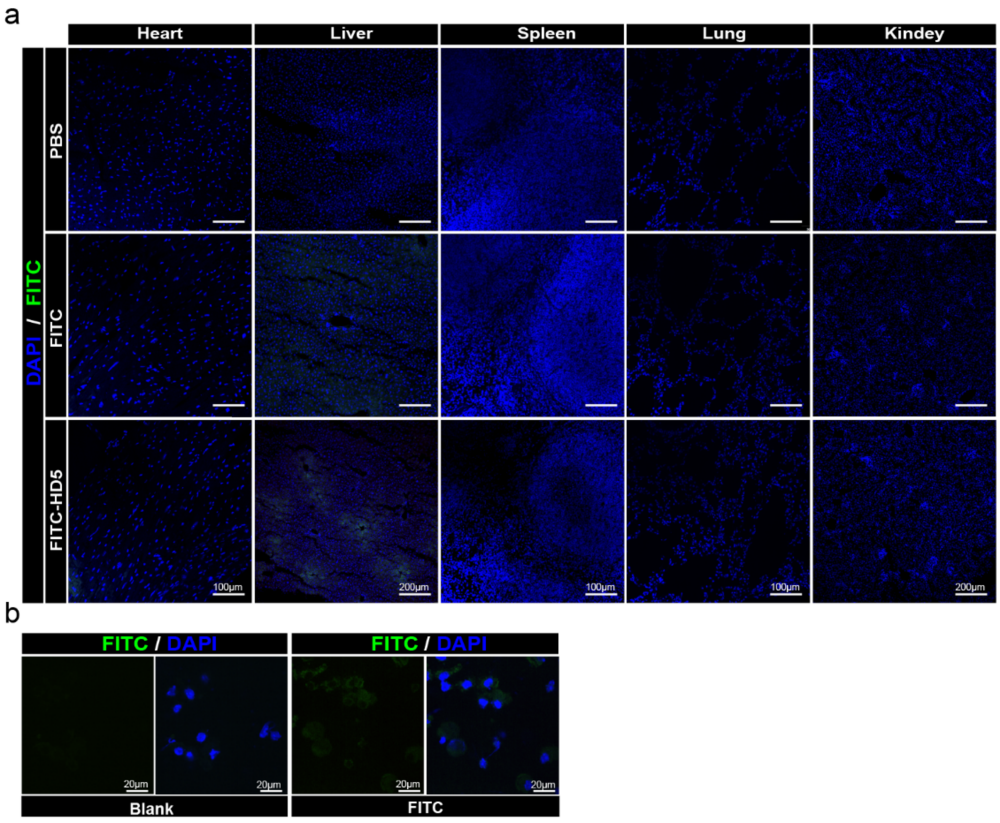

Supplementary Figure 2. Pharmacological distribution of FITC-D3 in other major viscera. a, Confocal images of sections from heart, liver, spleen, lung and kidney of SPF mice, three hours after oral administration of D3. Scale bars: 100/200 μm. **b**, Localization of FITC or FITC-D3 visualized by confocal microscopy. HCT 166 cells were incubated with 10 μM FITC and FITC-D3 (green) for 2 hours. Scale bars: 20 μm. Images are representative of three independent experiments with similar results.

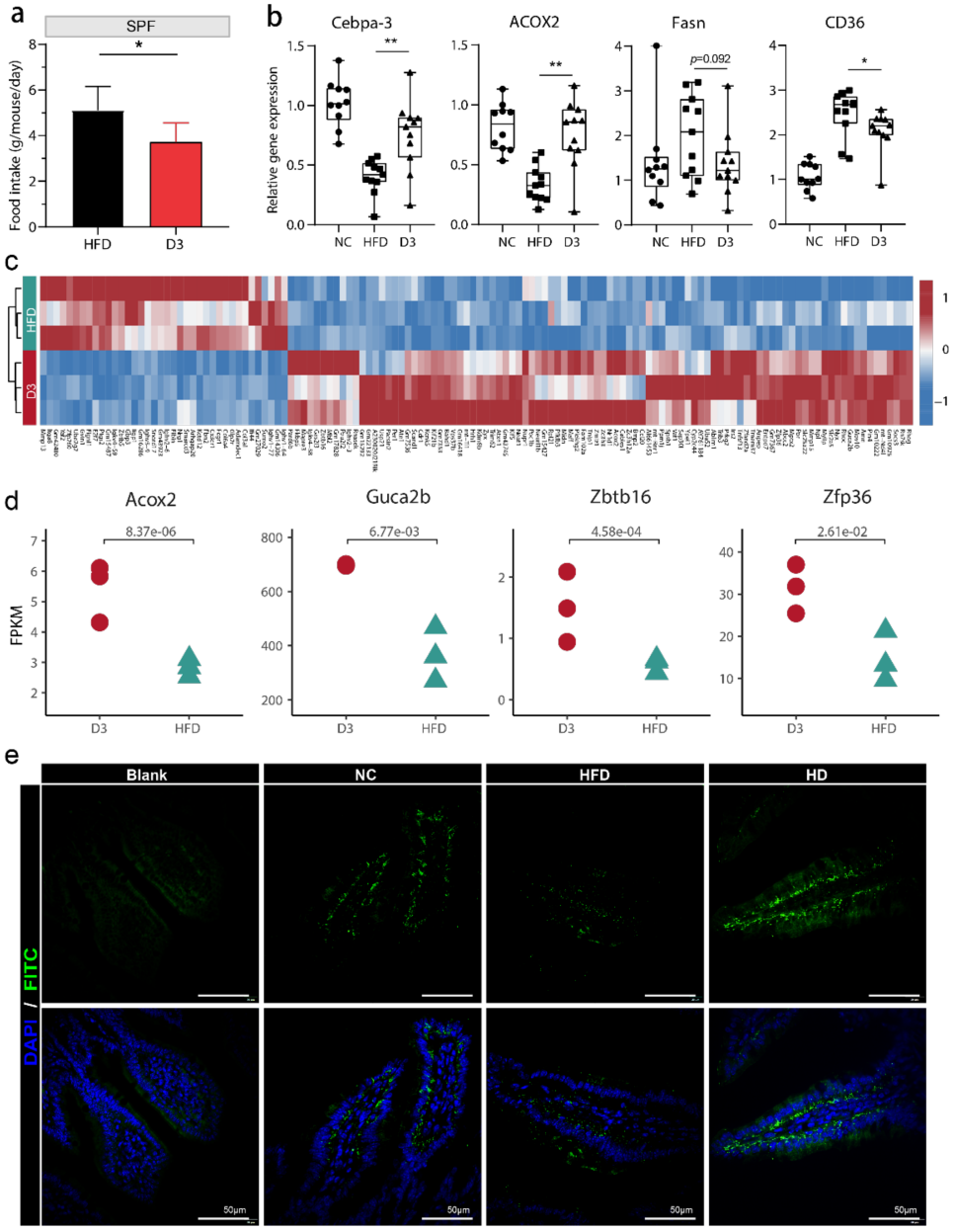

Supplementary Figure 3. Differentially expressed genes and immunofluorescence of UGN in ileum. a, Effect of D3 treatment on acute food intake, which was measured every other day for one week (SPF mice, n=10-12). **b**, Cebpa-3, Acox2, CD36 and Fasn (epididymis) mRNA expression levels of mice fed a control diet (NC and HFD) or treated with D3 (SPF mice, n=10-12). For **a** and **b**, *P* values were determined by a two-tailed Wilcoxon test, and data are presented as the means ± s.e.m; $P < 0.05$ (*); $P < 0.01$ (**). **c**, Clustering differentially expressed (DE) genes between HFD and D3. Different rows represent different samples and different columns represent DE genes. Relative levels of gene expression are depicted with a color scale in which red represents the highest level of up-regulated expression and blue represents the lowest level of down-

regulated expression. **d**, The relative expression levels of Acox2, Guca2b, Zfp36 and Zbtb16. P values were determined by two-tailed Wilcoxon test**. e**, Higher multiples of immunofluorescence in ileum sections for UGN (UGN, green) and nuclei (blue), while the diffuse green thin layer is a noisy background. Scale bars, 50 μm. Images are representative of three independent experiments with similar results.

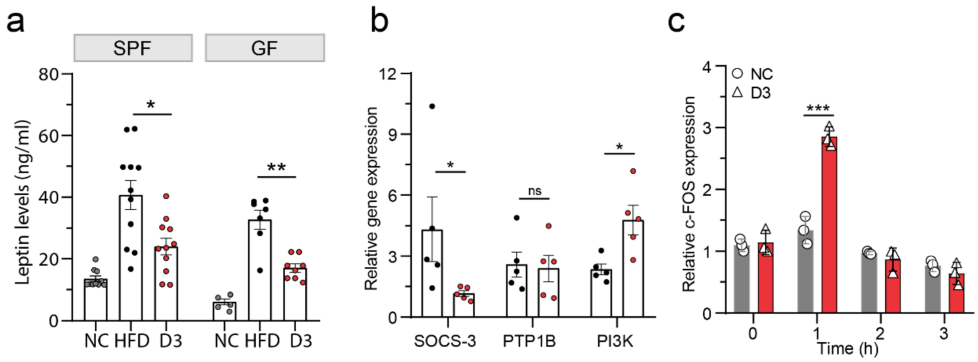

Supplementary Figure 4. D3 increases leptin sensitivity in mice. a, The concentration of leptin (ng/mL) in the serum of mice was determined by ELISA. **b**, mRNA expression level s of SOCS-3, PTP1B and PI3K of arcuate nucleus in mice of pair-feeding assay. **c**, mRNA expression levels of c-FOS. *P* values were determined by a two-tailed Wilcoxon test, and data are presented as the means ± s.e.m*; P* < 0.05 (*); *P* < 0.01 (**); *P* < 0.001 (***).

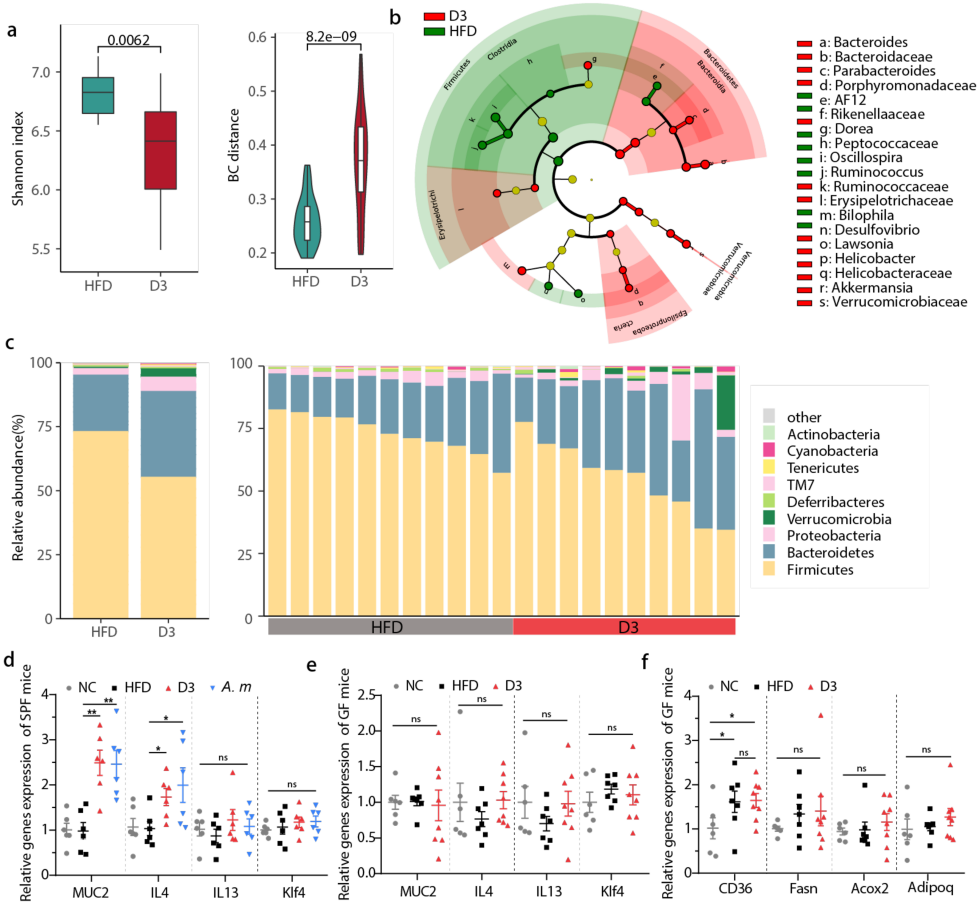

Supplementary Figure 5. Altered gut microbiota by D3 can affect gene expression in ileum of mice. a, Microbial diversity of the gut microbiota in mice, and the Bray-Curtis (BC) distance of the microbial communities between different groups. **b**, Cladogram representing significantly enriched taxa in D3 (red) or HFD (green). **c**, Fecal microbiota composition in HFD and D3 treated mice at a phylum level. The two bars on the left show the average relative abundance of each phylum. **d**, MUC2, IL4, IL13, and Klf4 mRNA expression levels in the colon of SPF mice fed on control diet (NC and HFD) or treated with D3 or gavaged with *A. muciniphila* (n = 6 mice per group). **e**, MUC2, IL4, IL13, and Klf4 mRNA expression levels in the colon of GF mice fed on control diet (NC and HFD) or treated with D3 (n = 6-8 mice per group). **f**, CD36, Fasn and Acox2 (liver) and Adipoq (epididymis) mRNA expression levels of GF mice fed on control diet (NC and HFD) or treated with D3 (n = 6 mice per group). *P* values were determined by two-tailed Wilcoxon test and data are presented as means ± s.e.m; *P* >0.05 (ns); *P* <0.05 (*); *P* <0.01 (**).

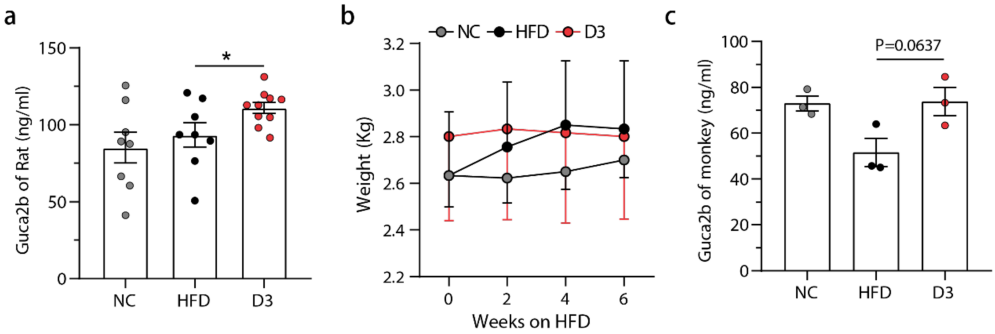

Supplementary Figure 6. Altered gut microbiota by D3 can affect gene expression in ileum of mice. a, The concentration of UGN (ng/mL) in the serum of rat was determined by ELISA. **b**, Kilograms of weight gain measured over time (n=3 macaques per group). **c**, The concentration of UGN (ng/mL) in the serum of macaques was determined by ELISA *P* values were determined by two-tailed Wilcoxon test and data are presented as means ± s.e.m; $P > 0.05$ (ns); $P < 0.05$ (*).

Supplementary Table 1. Physicochemical properties of peptides.

Peptide	HD5(1-9)	D1	D2	D3	D4
Charge	2	2	3	4	3
Prob of N-in[a]	0.91230	0.93899	0.93899	0.96573	0.95136

[a] Total prob of N-in: The total probability that the N-term is on the cytoplasmic side of the membrane.

Supplementary Table 2. The primers used in qPCR analysis.

Target	Primer	Sequence (5'-3')
Guca2b	Forward	GTACAGGCTGCTGATGAAATGAC
	Reverse	GGATGGCGATTACTTCAATGGTG
Leptin	Forward	TCTGAAAGATCCCACGTGCC
	Reverse	GGCTCAGGACATTCCAGCTT
CD36	Forward	GACGTGGCAAAGAACAGCAG
	Reverse	ATGGCTCCATTGGGCTGTAC
Fasn	Forward	AGCAGTATGTGACCACTGTGAG
	Reverse	TGATCCTCCTCTTCCAAGCAAC
Acox2	Forward	AGGCCATGTCTTCAGACTTCTG
	Reverse	CCTCATACGTGCAAGAGGCTAT
Adipoq	Forward	CCTGGCCACTTTCTCCTCATT
	Reverse	AAGAGGAACAGGAGAGCTTGC
Klf4	Forward	AGGAACTCTCTCACATGAAGC
	Reverse	CCTCTCTTGCTCAGTGTCCT
IL4	Forward	TGAGTCCAAGTCCACATCACTG
	Reverse	GGTCGTTGAACTCCTCGGTC
IL13	Forward	TCTCCCTCTGACCCTTAAGGAG
	Reverse	AGAGGCCATGCAATATCCTCTG
MUC2	Forward	AGGGCTCGGAACTCCAGAAA
	Reverse	CCAGGGAATCGGTAGACATCG
GAPDH	Forward	AACAGCAACTCCCACTCTTC
	Reverse	CCTCTCTTGCTCAGTGTCCT
Igrm1	Forward	CTTTCCCAATGTGGTGCTGTG
	Reverse	AACCTCTTTCCCATGCTCTGG
IFN-γ	Forward	CCACGGCACAGTCATTGAAAG
	Reverse	TGCTGATGGCCTGATTGTCTT
16S RNA	1369F	CGGTGAATACGTTCYCGG
	1492R	GGWTACCTTGTTACGACTT
A. muciniphila	Forward	CAGCACGTGAAGGTGGGGAC
	Reverse	CCTTGCGGTTGGCTTCAGAT

Cebpa-3	Forward	AGAACAGCAACGAGTACCGG
	Reverse	TGGTCAACTCCAGCACCTTC
C-FOS	Forward	TGGATTTGACTGGAGGTCTGC
	Reverse	CGTTGCTGATGCTCTTGACTG
AgRP	Forward	CTTCCACCTTTGCAGCATTCC
	Reverse	ACACGTGACTGCTTCCTGTAG
POMC	Forward	ATGCCGAGATTCTGCTACAGTC
	Reverse	CACCAGCTCCACACATCTATGG
PI3K	Forward	CTGAAGGCTATAAACGTGCAGC
	Reverse	CCTTTCTGGCATCCTGTACACT
PTP1B	Forward	CCCATCTTCCGTGGACATCAA
	Reverse	AGAGCTCCTTCCACTGATCCT
SOCS-3	Forward	ACTCTGACTCTACACTCGCCT
	Reverse	CGTGAAGTCTACAAAGGGGCT
NR2B	Forward	CCATGAACGAGACTGACCCAA
	Reverse	GAAATCGAGGATCTGGGCGAT
UCP-1	Forward	TGACTATGGTGCGCACAGAG
	Reverse	CTGCCACACCTCCAGTCATT
UCP-3	Forward	GATACATGAACGCTCCCCTAGG
	Reverse	GGCCCTCTTCAGTTGCTCATAT
Prdm16	Forward	AATGGACAAACGGCCTGAGAT
	Reverse	AATGGACAAACGGCCTGAGAT
CIDEA	Forward	GATGCACAAGCTTCAAGGCC
	Reverse	TGTATCGCCCAGTACTCGGA
Pgc1a	Forward	AGCCGTGACCACTGACAACGAG
	Reverse	AGCCGTGACCACTGACAACGAG
IL22	Forward	TCCCATCACAAGCAGAGACAC
	Reverse	TCCCATCACAAGCAGAGACAC
NR1D1	Forward	GGTGGTAGAGTTTGCCAAACAC
	Reverse	GGTGGTAGAGTTTGCCAAACAC
IL6	Forward	CTGCAAGAGACTTCCATCCAGT
	Reverse	CTGCAAGAGACTTCCATCCAGT
IL1β	Forward	AGGCTGACAGACCCCAAAAG
	Reverse	AGGCTGACAGACCCCAAAAG
TNF-α	Forward	CTGTGCCTCAGCCTCTTCTC
	Reverse	CTGTGCCTCAGCCTCTTCTC

1 Everard A, Lazarevic V, Derrien M, *et al.* Responses of Gut Microbiota and Glucose and Lipid Metabolism to Prebiotics in Genetic Obese and Diet-Induced Leptin-Resistant Mice. Diabetes

2011;**60**:2775-86.

2 Cheng YC, Liu JR. Effect of Lactobacillus rhamnosus GG on Energy Metabolism, Leptin Resistance, and Gut Microbiota in Mice with Diet-Induced Obesity. Nutrients 2020;**12**.

3 Folgueira C, Beiroa D, González-Rellán MJ*, et al.* Uroguanylin Improves Leptin Responsiveness in Diet-Induced Obese Mice. Nutrients 2019;**11**:752.

4 de Lartigue G, Barbier de la Serre C, Espero E*, et al.* Diet-induced obesity leads to the development of leptin resistance in vagal afferent neurons. American journal of physiology Endocrinology and metabolism 2011;**301**:E187-E95.

5 Kim GW, Lin JE, Snook AE*, et al.* Calorie-induced ER stress suppresses uroguanylin satiety signaling in diet-induced obesity. Nutr Diabetes 2016;**6**:e211.

6 Sato S, Basse AL, Schönke M*, et al.* Time of Exercise Specifies the Impact on Muscle Metabolic Pathways and Systemic Energy Homeostasis. Cell Metabolism 2019;**30**:92-110.e4.

7 Bibiloni R, Waget A, Neyrinck AM*, et al.* Changes in gut microbiota control metabolic endotoxemia-induced inflammation in high-fat diet-induced obesity and diabetes in mice.

8 Cani PD, Amar J, Iglesias MA*, et al.* Metabolic Endotoxemia Initiates Obesity and Insulin Resistance. Diabetes 2007;**56**:1761.

9 Everard A, Belzer C, Geurts L*, et al.* Cross-talk between Akkermansia muciniphila and intestinal epithelium controls diet-induced obesity. Proc Natl Acad Sci U S A 2013;**110**:9066-71.

10 Pertea M, Kim D, Pertea GM*, et al.* Transcript-level expression analysis of RNA-seq experiments with HISAT, StringTie and Ballgown. Nature protocols 2016;**11**:1650.

11 Walter W, Sánchez-Cabo F, Ricote M. GOplot: an R package for visually combining expression data with functional analysis. Bioinformatics 2015;**31**:2912-4.